

## Article

# Anthraquinones, Diphenyl Ethers, and Their Derivatives from the Culture of the Marine Sponge-Associated Fungus *Neosartorya spinosa* KUFA 1047<sup>†</sup>

Joana D. M. de Sá<sup>1</sup> , José A. Pereira<sup>2,3</sup> , Tida Dethoup<sup>4</sup>, Honorina Cidade<sup>1,3</sup> , Maria Emília Sousa<sup>1,3</sup> ,  
Inês C. Rodrigues<sup>2</sup>, Paulo M. Costa<sup>2,3</sup> , Sharad Mistry<sup>5</sup>, Artur M. S. Silva<sup>6</sup>  and Anake Kijjoo<sup>2,3,\*</sup> 

- <sup>1</sup> Laboratório de Química Orgânica, Departamento de Ciências Químicas, Faculdade de Farmácia, Universidade do Porto, Rua de Jorge Viterbo Ferreira, 228, 4050-313 Porto, Portugal; joanadmsa2703@gmail.com (J.D.M.d.S.); hcidade@ff.up.pt (H.C.); esousa@ff.up.pt (M.E.S.)
- <sup>2</sup> ICBAS—Instituto de Ciências Biomédicas Abel Salazar, Rua de Jorge Viterbo Ferreira, 228, 4050-313 Porto, Portugal; jpereira@icbas.up.pt (J.A.P.); inescoutorodrigues@gmail.com (I.C.R.); pmcosta@icbas.up.pt (P.M.C.)
- <sup>3</sup> Interdisciplinary Centre of Marine and Environmental Research (CIIMAR), Terminal de Cruzeiros do Porto de Leixões, Av. General Norton de Matos s/n, 4450-208 Matosinhos, Portugal
- <sup>4</sup> Department of Plant Pathology, Faculty of Agriculture, Kasetsart University, Bangkok 10240, Thailand; tdethoup@yahoo.com
- <sup>5</sup> Department of Chemistry, University of Leicester, University Road, Leicester LE 7RH, UK; scm11@leicester.ac.uk
- <sup>6</sup> Departamento de Química & QOPNA, Universidade de Aveiro, 3810-193 Aveiro, Portugal; artur.silva@ua.pt
- \* Correspondence: ankijjoo@icbas.up.pt; Tel.: +351-22-042-8331; Fax: +351-22-206-2232
- <sup>†</sup> Dedicated to Prof. Peter Proksch, one of the pioneers of marine natural products research in Europe.



**Citation:** de Sá, J.D.M.; Pereira, J.A.; Dethoup, T.; Cidade, H.; Sousa, M.E.; Rodrigues, I.C.; Costa, P.M.; Mistry, S.; Silva, A.M.S.; Kijjoo, A. Anthraquinones, Diphenyl Ethers, and Their Derivatives from the Culture of the Marine Sponge-Associated Fungus *Neosartorya spinosa* KUFA 1047. *Mar. Drugs* **2021**, *19*, 457. <https://doi.org/10.3390/md19080457>

Academic Editors: Bin-Gui Wang, Chang-Yun Wang and RuAngelie Edrada-Ebel

Received: 20 July 2021

Accepted: 9 August 2021

Published: 11 August 2021

**Publisher's Note:** MDPI stays neutral with regard to jurisdictional claims in published maps and institutional affiliations.



**Copyright:** © 2021 by the authors. Licensee MDPI, Basel, Switzerland. This article is an open access article distributed under the terms and conditions of the Creative Commons Attribution (CC BY) license (<https://creativecommons.org/licenses/by/4.0/>).

**Abstract:** Previously unreported anthraquinone, acetylpenipurdin A (4), biphenyl ether, neospinosic acid (6), dibenzodioxepinone, and spinolactone (7) were isolated, together with (*R*)-6-hydroxymellein (1), penipurdin A (2), acetylquestinol (3), tenellic acid C (5), and vermioxocin A (8) from the culture of a marine sponge-associated fungus *Neosartorya spinosa* KUFA1047. The structures of the previously unreported compounds were established based on an extensive analysis of 1D and 2D NMR spectra as well as HRMS data. The absolute configurations of the stereogenic centers of 5 and 7 were established unambiguously by comparing their calculated and experimental electronic circular dichroism (ECD) spectra. Compounds 2 and 5–8 were tested for their in vitro acetylcholinesterase and tyrosinase inhibitory activities as well as their antibacterial activity against Gram-positive and Gram-negative reference, and multidrug-resistant strains isolated from the environment. The tested compounds were also evaluated for their capacity to inhibit biofilm formation in the reference strains.

**Keywords:** *Neosartorya spinosa*; Trichocomaceae; marine sponge-associated fungus; anthraquinones; biphenyl ethers; anti-tyrosinase; antibacterial activity; antibiofilm activity

## 1. Introduction

Fungi are among organisms that have a remarkable capacity to produce different classes of structurally diverse secondary metabolites with relevant biological and pharmacological activities. This capability may be due to their necessity to produce highly bioactive molecules for their communications or inhibition of the growth of antagonistic neighbor microorganisms with which they cohabit in the same ecological niches [1]. Although secondary metabolites of terrestrial fungi have been extensively investigated for many decades due to their importance in pharmaceutical research [2], only in the past two decades that marine-derived fungi started to gain more attention from researchers [3]. Marine-derived fungi have become one of the most important sources of bioactive compounds not only because they are among the world's most important resources for unprecedented chemodiversity but also because they can produce quantity of compounds with potential for drug development, clinical trials, and even marketing [4].

In our research program with an objective to search for new bioactive compounds from marine-derived fungi, we investigated several members of the genus *Neosartorya* (Trichocomaceae) isolated from different marine organisms such as sponges, coral, and algae. Many different chemical classes of secondary metabolites, such as polyketides, isocoumarins, ergosterol derivatives, meroditerpenes, pyripropenes, benzoic acid derivatives, prenylated indole derivatives, tryptoquivalines, fiscalins, phenylalanine-derived alkaloids, and cyclopeptides, have been isolated and investigated for their anticancer and antibacterial activities [5–7]. Therefore, in our ongoing search for new natural antibiotics from marine-derived fungi, we investigated secondary metabolites from the culture of *N. spinosa* KUFA 1047, isolated from a marine sponge *Mycale* sp., which was collected from the Samae San Island in the Gulf of Thailand. Although the soil-derived *N. spinosa* has already been investigated for its secondary metabolites [8], this is the first study of the secondary metabolites from a marine-derived *N. spinosa*.

Fractionation of the ethyl acetate extract of the culture of *N. spinosa* KUFA 1047 by column chromatography of silica gel, followed by purification by preparative TLC, Sephadex LH-20 column, and crystallization led to the isolation of undescribed acetylpenipurdin A (4), neospinosic acid (6), and spinolactone (7), as well as the previously reported (*R*)-6-hydroxymellein (1) [9,10], penipurdin A (2) [11], acetylquestinol (3) [12], tenellic acid C (5) [13], and vermioxin A (8) [14–16] (Figure 1). The structures of the undescribed compounds were established based on an extensive analysis of their 1D and 2D NMR as well as HRMS spectra. In the case of 5 and 7, the absolute configurations of their stereogenic carbons were established by comparison of their experimental and calculated electronic circular dichroism (ECD) spectra.

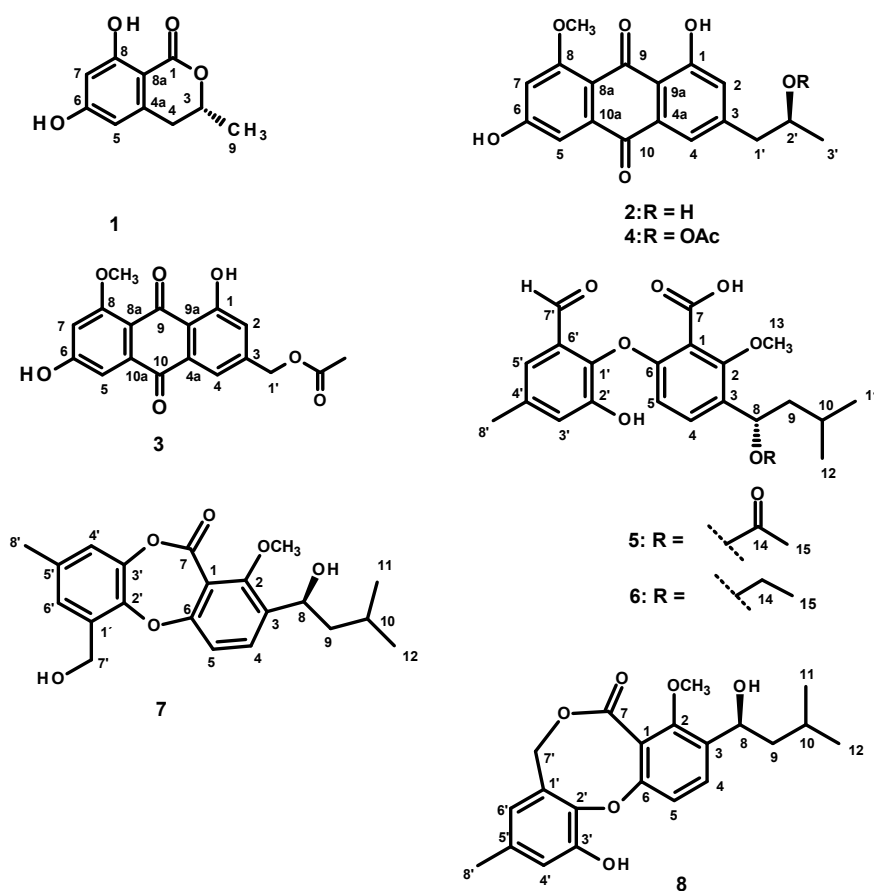


**Figure 1.** Structures of (*R*)-6-hydroxymellein (1), penipurdin A (2), acetylquestinol (3), acetylpenipurdin A (4), tenellic acid C (5), neospinosic acid (6), spinolactone (7), and vermioxin A (8).

Compounds **2** and **5–8** were tested for their in vitro acetylcholinesterase and tyrosinase inhibitory activities, as well as their antibacterial activity against Gram-negative and Gram-positive bacteria by disk diffusion and by determination of the minimum inhibitory concentration (MIC) and minimal bactericidal concentration (MBC) of several reference strains and environmental multidrug-resistant isolates. The tested compounds were also evaluated for their potential synergy with clinically relevant antibiotics on the multidrug-resistant isolates, by a disk diffusion method and by the checkerboard assay, as well as their capacity to prevent biofilm formation in all four reference strains, by measuring a total biomass using the crystal violet assay.

## 2. Results and Discussion

The structures of (*R*)-6-hydroxymellein (**1**) [9,10], penipurdin A (**2**) [11], acetylquestinol (**3**) [12], tenellic acid C (**5**) [13], and vermioxin A (**8**) [14–16] (Figure 1) were elucidated by analysis of their 1D and 2D NMR spectra as well as HRMS data, and also by comparison of their spectral data and signs of optical rotations (Figures S1–S25 and S38–S43, Tables S1–S5) with those reported in the literature.

Compounds **3** and **4** were isolated as a 1:3 mixture (estimated by the integration of protons in the  $^1\text{H}$  NMR spectrum). The molecular formula of the minor compound (**3**) was determined as  $\text{C}_{18}\text{H}_{14}\text{O}_7$  on the basis of its (+)-HRESIMS  $m/z$  343.0809  $[\text{M} + \text{H}]^+$  (calculated for  $\text{C}_{18}\text{H}_{15}\text{O}_7$ , 343.0818), while the molecular formula of the major compound (**4**) was established as  $\text{C}_{20}\text{H}_{18}\text{O}_7$  on the basis of (+)-HRESIMS  $m/z$  371.1124  $[\text{M} + \text{H}]^+$  (calculated for  $\text{C}_{20}\text{H}_{19}\text{O}_7$ , 371.1131) (Figures S18 and S19). The  $^1\text{H}$  and  $^{13}\text{C}$  signals as well as correlations observed in the COSY, HSQC, and HMBC spectra of a minor component (Table S3, Figures S13–S17) revealed its identity as acetylquestinol, previously reported from the culture of *Eurotium chevalieri* KUFA0006 [12].

The  $^{13}\text{C}$  NMR spectrum (Table 1, Figure S14) of the major compound (**4**) showed 20 carbon signals, which, in combination with DEPT and HSQC spectra (Figure S16), can be categorized as two conjugated ketone carbonyls ( $\delta_{\text{C}}$  186.4 and 183.0), one ester carbonyl ( $\delta_{\text{C}}$  170.2), three oxygen-bearing  $\text{sp}^2$  ( $\delta_{\text{C}}$  166.6, 164.1, 162.1), five non-protonated  $\text{sp}^2$  ( $\delta_{\text{C}}$  146.6, 137.2, 132.6, 115.6, 112.2), four protonated  $\text{sp}^2$  ( $\delta_{\text{C}}$  125.1, 119.6, 108.3, 105.5), one oxygen-bearing methine  $\text{sp}^3$  ( $\delta_{\text{C}}$  70.7), one methoxy ( $\delta_{\text{C}}$  56.7), one methylene  $\text{sp}^2$  ( $\delta_{\text{C}}$  41.5), and two methyl ( $\delta_{\text{C}}$  21.4 and 20.0) carbons. The  $^1\text{H}$  NMR spectrum (Figure S13), in conjunction with COSY and HMBC spectra (Table 1, Figures S15 and S17), showed the following proton signals: a singlet of a hydrogen-bonded phenolic hydroxyl proton at  $\delta_{\text{H}}$  13.40, two pairs of *meta*-coupled aromatic protons at  $\delta_{\text{H}}$  7.15, d ( $J = 1.5$  Hz,  $\delta_{\text{C}}$  125.1)/ $\delta_{\text{H}}$  7.47, d ( $J = 1.5$  Hz,  $\delta_{\text{C}}$  119.6) and  $\delta_{\text{H}}$  7.16, d ( $J = 2.2$  Hz,  $\delta_{\text{C}}$  108.3)/ $\delta_{\text{H}}$  6.78, d ( $J = 2.2$  Hz,  $\delta_{\text{C}}$  105.5), a multiplet at  $\delta_{\text{H}}$  5.06 ( $\delta_{\text{C}}$  70.7), a methoxyl singlet at  $\delta_{\text{H}}$  3.89 ( $\delta_{\text{C}}$  56.7), a multiplet at  $\delta_{\text{H}}$  2.92 ( $\delta_{\text{C}}$  41.5), a methyl singlet at  $\delta_{\text{H}}$  1.94 ( $\delta_{\text{C}}$  21.4), and a methyl doublet at  $\delta_{\text{H}}$  1.20, d ( $J = 6.3$  Hz,  $\delta_{\text{C}}$  20.0). The general feature of the  $^1\text{H}$  and  $^{13}\text{C}$  NMR spectra of **4** resembled those of **2** [11], except for the presence of the ester carbonyl at  $\delta_{\text{C}}$  170.2 and a methyl singlet at  $\delta_{\text{H}}$  1.94 ( $\delta_{\text{C}}$  21.4), characteristic of an acetyl group. That the substituent on C-3 was 2-acetoxypropyl instead of 2-hydroxypropyl in **2** was evidenced by the COSY correlations from H<sub>2</sub>-1' ( $\delta_{\text{H}}$  2.92, m/ $\delta_{\text{C}}$  41.5) to H-2' ( $\delta_{\text{H}}$  5.06/ $\delta_{\text{C}}$  70.7), and from H-2' to H<sub>3</sub>-3' ( $\delta_{\text{H}}$  1.20, d,  $J = 6.3$  Hz/ $\delta_{\text{C}}$  20.0) as well as by HMBC correlations from H-2' and a methyl singlet at  $\delta_{\text{H}}$  1.94 ( $\delta_{\text{C}}$  21.1) to the carbonyl at  $\delta_{\text{C}}$  170.2, H-1' to C-2, C-3 ( $\delta_{\text{C}}$  146.6), C-4, and from H-2' to C-3.

**Table 1.**  $^1\text{H}$  and  $^{13}\text{C}$  NMR (DMSO- $d_6$ , 500 and 125 MHz) and HMBC assignment for **4**.

Position	$\delta_{\text{C}}$ , Type	$\delta_{\text{H}}$ , $J$ in Hz	COSY	HMBC
1	162.1, C			
2	125.1, CH	7.15, d (1.5)	H-4	C-1, 1', 4, 9a
3	146.6, C			
4	119.6, CH	7.47, d (1.5)	H-2	C-1', 2, 9a, 10
4a	132.6, C			
5	108.3, CH	7.16, d (2.2)	H-7	C-7, 8a, 10
6	166.6, C			
7	105.5, CH	6.78, d (2.2)	H-5	C-5, 6, 8a
8	164.1, C			
8a	112.2, C			
9	186.4, CO			
9a	115.6, C			
10	183.0, CO			
10a	137.2, C			
OMe-8	56.7, CH <sub>3</sub>	3.89, s		C-8
1'	41.5, CH <sub>2</sub>	2.92, m	H-2'	C-2, 3, 4
2'	70.7, CH	5.06, m	H <sub>2</sub> -1', H <sub>3</sub> -3'	C-3, CO (Ac)
3'	20.0, CH <sub>3</sub>	1.20, d (6.3)	H-2'	C-1', 2'
CO (Ac)	170.2, CO			
Me (Ac)	21.4, CH <sub>3</sub>	1.94, s		
OH-1'	-	13.40, s		C-1, 2, 9a

The optical rotation of a mixture of **3** and **4** is dextrorotatory, with  $[\alpha]_{\text{D}}^{20} + 142.8$  ( $c$  0.035, MeOH). Since **3** is not a chiral molecule, only **4** is responsible for the optical activity. The structure of **4** corresponds to an acetylated derivative of **2** ( $[\alpha]_{\text{D}}^{20} + 35.7$  ( $c$  0.033, MeOH; Lit. + 33 ( $c$  1.14, MeOH)) and is, therefore, named acetylpenipurdin A. Based on the biogenetic consideration, the absolute configuration of C-2' in **4** should be the same as that of C-2' in **2**, i.e., (*S*). Additionally, this hypothesis was supported by the same sign of their optical rotations (dextrorotatory), which is based on the report by Singh et al. [17], that 1,3,8-trihydroxy-6-(2'-acetoxyptopyl) anthracene-9,10-dione, isolated from the marine crinoid *Pterometra venusta*, ( $[\alpha]_{\text{D}}^{25} + 40$ ,  $c$  0.05, MeOH) and its deacetylated product ( $[\alpha]_{\text{D}}^{25} + 37$ ,  $c$  0.05, MeOH) were both dextrorotatory. Literature search revealed that **4** has never been previously reported.

The (+)-HRESIMS,  $^1\text{H}$  and  $^{13}\text{C}$  NMR data (Table S4, Figures S20 and S21) of **5** ( $[\alpha]_{\text{D}}^{20} - 7.8$  ( $c$  0.079, MeOH)) are compatible with those of tenellic acid C ( $[\alpha]_{\text{D}}^{25} - 7.4$  ( $c$  0.13 g/dL, MeOH)), a biphenyl ether derivative isolated from the aquatic fungus *Dendrospora tenella* [13]; however, the absolute configuration of C-8 was not established. To determine the absolute configuration of C-8, the experimental ECD spectrum of **5** was measured and then compared with a quantum-mechanically simulated spectrum derived from the most significant computational models of (*S*)-**5** (Figure 2, please see the Experimental section for details). Figure 3 shows the visual match between experimental and calculated ECD spectra, with the spectrum of the (*8S*) configuration mostly in phase with the experimental spectrum, while the spectrum of (*8R*) configuration is mostly out of phase, leading to an unambiguous conclusion that the absolute configuration of C-8 is (*S*).

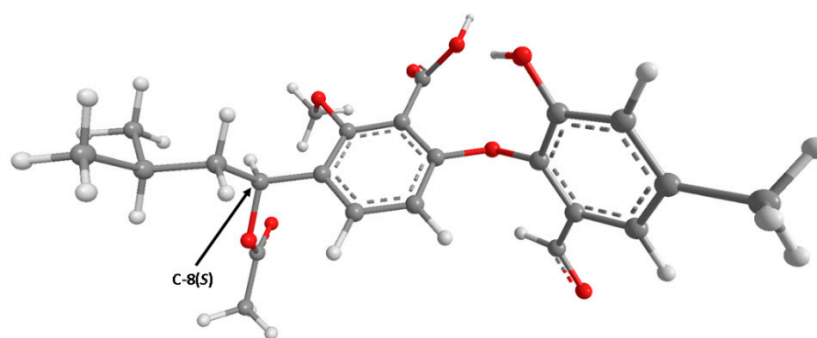


**Figure 2.** Model of one of the most abundant conformations of **5** (lowest B3LYP/6-31G/methanol energy conformer) in its ECD assigned (8S) configuration. Many other conformations have very similar energies to this one.

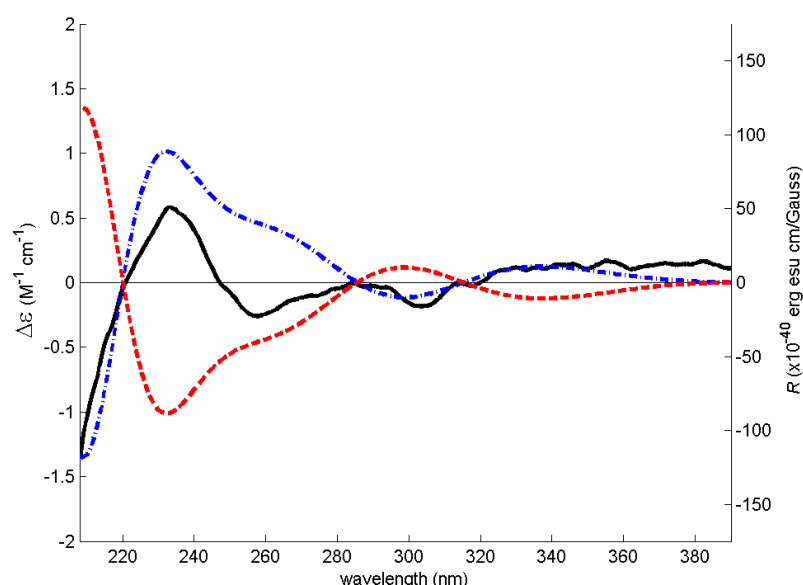


**Figure 3.** Experimental methanol ECD spectrum of **5** (solid black line) and theoretical ECD spectra of its (S) (dot-dashed blue line) and (R) (dashed red line) computational conformers.

Compound **6** was isolated as an amorphous yellow solid, and its molecular formula  $C_{23}H_{28}O_7$  was established based on the (+)-HRESIMS  $m/z$  417.1915  $[M + H]^+$  (calculated for  $C_{23}H_{29}O_7$ , 417.1913) (Figure S31), requiring 10 degrees of unsaturation. The general feature of the  $^1H$  and  $^{13}C$  NMR spectra of **6** resembled those of **5**. The  $^{13}C$  NMR spectrum (Table 2, Figure S27) exhibited 23 carbon signals, which can be categorized, according to DEPT and HSQC spectra (Figure S29), as one aldehyde carbonyl ( $\delta_C$  189.8), one conjugated carboxy carbonyl ( $\delta_C$  167.2), four oxygen-bearing  $sp^2$  ( $\delta_C$  155.1, 154.8, 150.9, and 142.3), four non-protonated  $sp^2$  ( $\delta_C$  136.7, 130.5, 129.8, and 119.3), four protonated  $sp^2$  ( $\delta_C$  128.5, 124.2, 118.4, and 110.3), one oxymethine  $sp^3$  ( $\delta_C$  73.1), one oxymethylene  $sp^3$  ( $\delta_C$  63.9), one methoxy ( $\delta_C$  62.8), one methylene  $sp^3$  ( $\delta_C$  47.1), one methine  $sp^3$  ( $\delta_C$  24.9), and four methyl ( $\delta_C$  23.7, 22.2, 21.0, and 15.7) carbons. The  $^1H$  NMR spectrum (Figure S26), in combination with the COSY spectrum (Table 2, Figure S28), displayed a singlet of an aldehyde proton at  $\delta_H$  10.15, the signals of two *ortho*-coupled aromatic protons at  $\delta_H$  7.25, d ( $J = 8.7$  Hz) and 6.32, d ( $J = 8.7$  Hz), two *meta*-coupled aromatic protons at  $\delta_H$  7.14, d ( $J = 2.0$  Hz) and 7.11, d ( $J = 2.0$  Hz), a double doublet at  $\delta_H$  4.58 ( $J = 9.2, 3.8$  Hz), a methoxy singlet at  $\delta_H$  3.83, a quartet at  $\delta_H$  3.25 ( $J = 7.0$  Hz), two double of double doublets of two geminally coupled methylene protons at  $\delta_H$  1.57 ( $J = 13.8, 9.1, 5.0$  Hz) and 1.27 ( $J = 13.8, 8.9, 3.9$  Hz), a multiplet at  $\delta_H$  1.71, one methyl singlet at  $\delta_H$  2.31, one methyl triplet at  $\delta_H$  1.06 ( $J = 7.0$  Hz), and two methyl doublets at  $\delta_H$  0.88 ( $J = 6.6$  Hz) and 0.92 ( $J = 6.6$  Hz). The  $^{13}C$  and  $^1H$  chemical

shift values and multiplicities of the proton signals revealed that **6** is also a biphenyl ether derivative. Like **5**, one of the benzene ring is 1,2,3,5-tetrasubstituted and another is 1,2,3,4-tetrasubstituted. That the 1,2,3,5-tetrasubstituted benzene ring has a formyl group on C-1', a hydroxyl group on C-3', and a methyl group on C-5' was corroborated by COSY correlations from the doublet at  $\delta_{\text{H}}$  7.14 ( $J = 2.0$  Hz, H-4'/ $\delta_{\text{C}}$  124.2) to the doublet at  $\delta_{\text{H}}$  7.11 ( $J = 2.0$  Hz, H-6'/ $\delta_{\text{C}}$  118.4) and the methyl singlet at  $\delta_{\text{H}}$  2.31 (Me-8'/ $\delta_{\text{C}}$  21.0), from Me-8' to H-4' and H-6' as well as HMBC correlations (Figure S30) from H-4' to C-6', C-8', C-2' ( $\delta_{\text{C}}$  142.3), and C-3' ( $\delta_{\text{C}}$  150.9), H-6' to C-2', C-7' ( $\delta_{\text{C}}$  189.8), and C-8', Me-8' to C-4', C-5' ( $\delta_{\text{C}}$  136.7), and C-6', H-7' ( $\delta_{\text{H}}$  10.15, s) to C-1' ( $\delta_{\text{C}}$  129.8) C-5' and C-6'. That another benzene ring has a carboxyl substituent on C-1, a methoxyl group on C-2, and an alkyl sidechain on C-3 was substantiated by COSY correlations from H-4 ( $\delta_{\text{H}}$  7.25, d,  $J = 8.7$  Hz/ $\delta_{\text{C}}$  128.5) to H-5 ( $\delta_{\text{H}}$  6.32, d,  $J = 8.7$  Hz/ $\delta_{\text{C}}$  110.3) as well as HMBC correlations from H-4 to C-2 ( $\delta_{\text{C}}$  155.1), C-6 ( $\delta_{\text{C}}$  154.8) and C-8 ( $\delta_{\text{C}}$  73.1), H-5 to C-1 ( $\delta_{\text{C}}$  119.3), C-3 ( $\delta_{\text{C}}$  130.5), C-6 and C-7 ( $\delta_{\text{C}}$  167.2), the methoxyl singlet at  $\delta_{\text{H}}$  3.83 ( $\delta_{\text{C}}$  62.8) to C-2. That the substituent on C-3 is 1-ethoxy-3-methylbutyl is corroborated by COSY correlations from H-8 ( $\delta_{\text{H}}$  4.58, dd,  $J = 9.2$ , 3.8 Hz/ $\delta_{\text{C}}$  73.1) to H<sub>2</sub>-9 ( $\delta_{\text{H}}$  1.57, ddd,  $J = 13.8$ , 9.1, 5.0 Hz and 1.27, ddd,  $J = 13.8$ , 8.9, 3.9 Hz/ $\delta_{\text{C}}$  47.1), H<sub>2</sub>-9 to H-10 ( $\delta_{\text{H}}$  1.71, m/ $\delta_{\text{C}}$  24.9), H-10 to Me-11 ( $\delta_{\text{H}}$  0.88, d,  $J = 6.6$  Hz/ $\delta_{\text{C}}$  23.7) and Me-12 ( $\delta_{\text{H}}$  0.92, d,  $J = 6.6$  Hz/ $\delta_{\text{C}}$  22.2), and H-14 ( $\delta_{\text{H}}$  3.25, q,  $J = 7.0$  Hz/ $\delta_{\text{C}}$  63.9) to Me-15 ( $\delta_{\text{H}}$  1.06, t,  $J = 7.0$  Hz/ $\delta_{\text{C}}$  15.7). This was supported by HMBC correlations from H-8 to C-9, C-14 and C-3, H-14 to C-8, Me-15, H-9 to C-8, C-11, Me-11 to C-9, C-10, C-12, and Me-12 to C-9, C-10 and C-11.

**Table 2.**  $^1\text{H}$  and  $^{13}\text{C}$  NMR (DMSO-*d*<sub>6</sub>, 300 and 75 MHz) and HMBC assignment for **6**.

Position	$\delta_{\text{C}}$ , Type	$\delta_{\text{H}}$ , ( $J$ in Hz)	COSY	HMBC
1	119.3, C	-		
2	155.1, C	-		
3	130.5, C			
4	128.5, CH	7.25, d (8.7)	H-5	C-2, 6, 8
5	110.3, CH	6.32, d (8.7)	H-4	C-1, 3, 6, 7 (w)
6	154.8, C	-		
7	167.2, CO	-		
8	73.1, CH	4.58, dd (9.2, 3.8)	H-9a, 9b	C-3, 9, 14
9a, b	47.1, CH <sub>2</sub>	1.57, ddd (13.8, 9.2, 5.0) 1.27, ddd (13.8, 8.9, 3.9)		C-8, 9, 11, 12
10	24.9, CH	1.71, m	H-9a, 9b, 11, 12	
11	23.7, CH <sub>3</sub>	0.88, d (6.6)	H-10	C-9, 10, 12
12	22.2, CH <sub>3</sub>	0.92, d (6.6)	H-10	C.9, 10, 11
13	62.8, OMe	3.83, s		
14	63.9, CH <sub>2</sub>	3.25, q (7.0)	H-15	C-8, 15
15	15.7, CH <sub>3</sub>	1.06, t (7.0)	H-14	C-14
1'	129.8, C	-		
2'	142.3, C	-		
3'	150.9, C	-		
4'	124.2, CH	7.14, d (2.0)	H-6', 8'	C-2', 3', 6', 8'
5'	136.7, C	-		
6'	118.4, CH	7.11, d (2.0)	H-4', 6'	C-2', 3' (w), 7', 8'
7'	189.8, CHO	10.15, s		C-1', 5' (w), 6'
8'	21.0, CH <sub>3</sub>	2.31, s	H-4', 6'	

w = weak.

Taking together the molecular formula and the partial structures, the two substituted benzene rings must be connected by an ether bridge through C-6 and C-2', forming a biphenyl ether derivative. The only difference between the structure of **6** and that of **5** is that the acetoxy group on C-8 in **5** was replaced by the ethoxy group in **6**. Since **6** cannot be obtained as a suitable crystal for X-ray analysis, we attempted to determine the absolute configuration of C-8 of **6** by comparing the experimental and calculated ECD spectra.

Unfortunately, **6** does not produce an ECD spectrum at a concentration that normally gives a visible spectrum for other compounds of this series. Therefore, based on the biogenic consideration, we presume that the absolute configuration of C-8 in **6** is the same as that in **5**. Moreover, this hypothesis is supported by the fact that both **5** and **6** are levorotatory. Thus, the absolute configuration of C-8 in **6** was proposed as (*S*). Since **6** has not been previously reported, it was named neospinosic acid.

Compound **7** was isolated as a yellow viscous oil, and its molecular formula was established as  $C_{21}H_{24}O_6$  on the basis of (+)-HRESIMS  $m/z$  373.1652  $[M + H]^+$  (calculated for  $C_{21}H_{25}O_6$ , 373.1651) (Figure S37), corresponding to 10 degrees of unsaturation. The  $^{13}C$  NMR spectrum (Table 3, Figure S33) displayed 21 carbon signals, which, in combination with DEPT and HSQC spectra (Figure S35), can be categorized as nine non-protonated  $sp^2$  ( $\delta_C$  161.6, 160.2, 157.9, 145.9, 143.4, 138.3, 136.3, 135.6, and 114.3), four protonated  $sp^2$  ( $\delta_C$  132.8, 125.9, 119.9, and 115.6), one methoxy ( $\delta_C$  63.1), one oxymethine  $sp^3$  ( $\delta_C$  64.4), one methine  $sp^3$  ( $\delta_C$  24.8), one oxymethylene  $sp^3$  ( $\delta_C$  57.9), one methylene  $sp^3$  ( $\delta_C$  48.3), and three methyl ( $\delta_C$  23.9, 22.1, and 20.9) carbons. The  $^1H$  NMR spectrum (Figure S32), in combination with the COSY spectrum (Table 3, Figure S34), showed two *ortho*-coupled aromatic protons at  $\delta_H$  7.67, d ( $J = 8.6$  Hz) and 7.21, d ( $J = 8.6$  Hz), two *meta*-coupled aromatic protons at  $\delta_H$  7.12, d ( $J = 0.5$  Hz) and 7.11, brs, one triplet at  $\delta_H$  5.34 ( $J = 5.8$  Hz), one double of double doublet at  $\delta_H$  4.87 ( $J = 9.2, 4.9, 4.2$  Hz), two doublet at  $\delta_H$  4.72 ( $J = 5.7$  Hz) and 5.13 ( $J = 4.9$  Hz), a methoxy singlet at  $\delta_H$  3.76, two geminally coupled double of double doublets at  $\delta_H$  1.24 ( $J = 13.7, 9.2, 4.2$  Hz) and  $\delta_H$  1.44 ( $J = 13.7, 9.2, 4.9$  Hz), a multiplet at  $\delta_H$  1.72, one methyl singlet at  $\delta_H$  2.28, and two methyl doublets at  $\delta_H$  0.86 ( $J = 6.7$  Hz) and 0.90 ( $J = 6.7$  Hz). The  $^1H$  and  $^{13}C$  chemical shift values and multiplicities of the aromatic proton signals suggested the presence of two substituted benzene rings in the molecule. That one of the benzene ring is 1,2,3,4-tetrasubstituted, with a methoxyl group on C-2 and an oxygenated substituent on C-6, was evidenced by the COSY correlations (Table 3) from the doublet at  $\delta_H$  7.67 ( $J = 8.6$  Hz, H-4/ $\delta_C$  132.8) to another doublet at  $\delta_H$  7.21 ( $J = 8.6$  Hz, H-5/ $\delta_C$  115.6) as well as by HMBC correlations (Table 3, Figure S36) from H-4 to the carbons at  $\delta_C$  160.2 (C-6), 157.9 (C-2) and the oxymethine  $sp^3$  carbon at  $\delta_C$  64.4, H-5 to the carbons at  $\delta_C$  114.3 (C-1), 138.3 (C-3), C-6, a methoxyl singlet at  $\delta_H$  3.76 ( $\delta_C$  63.1) to C-2. The chemical shift value of C-1 suggested that it was substituted by a carbonyl group. That the substituent on C-3 is 1-hydroxy-3-methylbutyl was substantiated by COSY correlations (Table 3) from H-8 ( $\delta_H$  4.87, ddd,  $J = 9.2, 4.9, 4.2$  Hz/ $\delta_C$  64.4) to the double of double doublet at  $\delta_H$  1.44 ( $J = 13.7, 9.2, 4.9$  Hz, H-9b/ $\delta_C$  48.3) and a doublet at  $\delta_H$  5.13 ( $J = 4.9$  Hz, OH-8), and HMBC correlations (Table 3) from H-9b to C-8, OH-8 to C-9, the methyl doublet at  $\delta_H$  0.86 ( $J = 6.7$  Hz/ $\delta_C$  23.9; Me-11) to the carbon at  $\delta_C$  48.3 (C-9), 24.8 (C-10), 22.1 (Me-12), the doublet at 0.90 ( $J = 6.7$  Hz/ $\delta_C$  22.1; Me-12) to C-9, C-10 and Me-11.

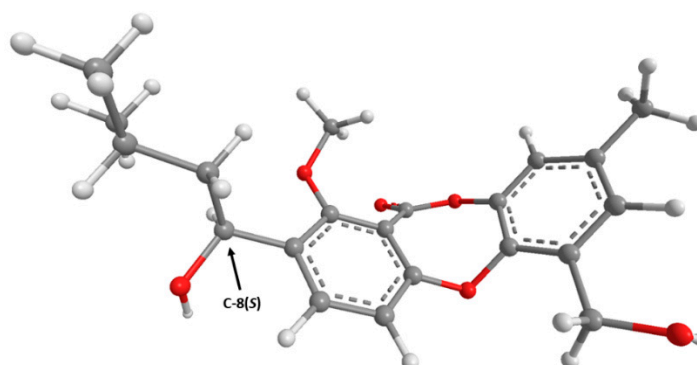
That another benzene ring is 1,2,3,5-tetrasubstituted, with a methyl substituent on C-5' and a hydroxymethyl group on C-1', was substantiated by a COSY correlation (Table 3) from the triplet at  $\delta_H$  5.34 ( $J = 5.8$  Hz, OH-7') to a doublet at  $\delta_H$  4.72 ( $J = 5.8$  Hz, H<sub>2</sub>-7'/ $\delta_C$  57.9) and HMBC correlations (Table 3) from H<sub>2</sub>-7' to the carbons at  $\delta_C$  125.9 (C-6'), 135.6 (C-1'), 145.9 (C-2'), the methyl singlet at  $\delta_H$  2.28 (Me-8'/ $\delta_C$  20.9) to the carbons at  $\delta_C$  119.9 (C-4'), 136.3 (C-5'), and C-6', a doublet at  $\delta_H$  7.12 ( $J = 0.5$  Hz, H-6'/ $\delta_C$  125.9) to C-4', C-2' ( $\delta_C$  145.9), C-7' and Me-8', and from a broad singlet at  $\delta_H$  7.11 (H-4'/ $\delta_C$  119.9) to C-2', C-3' ( $\delta_C$  143.4) and C-6'. The chemical shift values of C-2' and C-3' suggested that they are oxygen-bearing aromatic carbons.

Considering the  $^1H$  and  $^{13}C$  chemical shift values and the molecular formula, the two substituted benzene rings must be connected by an ether bridge between C-2' and C-6 as well as between the oxygen atom on C-3' and the carbonyl on C-1, thus forming a 5*H*-1,4-dioxepin-5-one ring. Therefore, the carbon at  $\delta_C$  161.6 was assigned to C-7.

**Table 3.**  $^1\text{H}$  and  $^{13}\text{C}$  NMR (DMSO- $d_6$ , 500 and 125 MHz) and HMBC assignment for 7.

Position	$\delta_{\text{C}}$ , Type	$\delta_{\text{H}}$ , (J in Hz)	COSY	HMBC
1	114.3, C	-		
2	157.9, C	-		
3	138.3, C	-		
4	132.8, CH	7.67, d (8.6)	H-5	C-1, 3, 6
5	115.6, CH	7.21, d (8.6)	H-4	C-2, 6, 8
6	160.2, C	-		
7	161.6, CO	-		
8	64.4, CH	4.87, ddd (9.2, 4.9, 4.2)	H-9a, 9b, OH-8	
9a, b	48.3, CH <sub>2</sub>	1.24, ddd (13.7, 9.2, 4.2)	H-8, 9b, 10	
		1.44, ddd (13.7, 9.2, 4.9)	H-8, 9a, 10	
10	24.8, CH	1.72, m	H-9a, b, Me	
			-11, 12	
11	23.9, CH <sub>3</sub>	0.86, d (6.7)	H-10	C-9, 12
12	22.1, CH <sub>3</sub>	0.90, d (6.7)	H-10	C-9, 11
13	63.1, OMe	3.76, s		C-2
1'	135.6, C	-		
2'	145.9, C	-		
3'	143.4, C	-		
4'	119.9, CH	7.11, brs		C-2', 3', 6'
5'	136.3, C	-		
6'	125.9, CH	7.12, d (0.5)		C-2', 4', 7', 8'
7'	57.9, CH <sub>2</sub>	4.72, d (5.8)	OH-7'	C-1', 2', 6'
8'	20.9, CH <sub>3</sub>	2.28, s		C-4', 5', 6'
OH-7'		5.34, t (5.8)	H-7'	C-7'
OH-8		5.13, d (4.9)	H-8	C-9

Since 7 has one stereogenic carbon (C-8), it is necessary to determine its absolute configuration. Compound 7 was isolated as a viscous oil, which was not able to determine the absolute configuration of C-8 by X-ray crystallography. Therefore, the absolute configuration of C-8 in 7 was determined by ECD. For this effect, the experimental ECD spectrum of 7 was measured and then compared with a quantum-mechanically simulated spectrum derived from the most significant computational models of (S)-7 (Figure 4; please see Experimental section for details). Figure 5 shows a good match between experimental and calculated ECD spectra, with the two spectra in phase, leading to a conclusion that the absolute configuration of C-8 is (S).

**Figure 4.** Model of the most abundant conformer of 7 (lowest B3LYP/6-31G/acetonitrile energy conformer) accounting for 48% of conformer population) in its ECD assigned (8S) configuration.

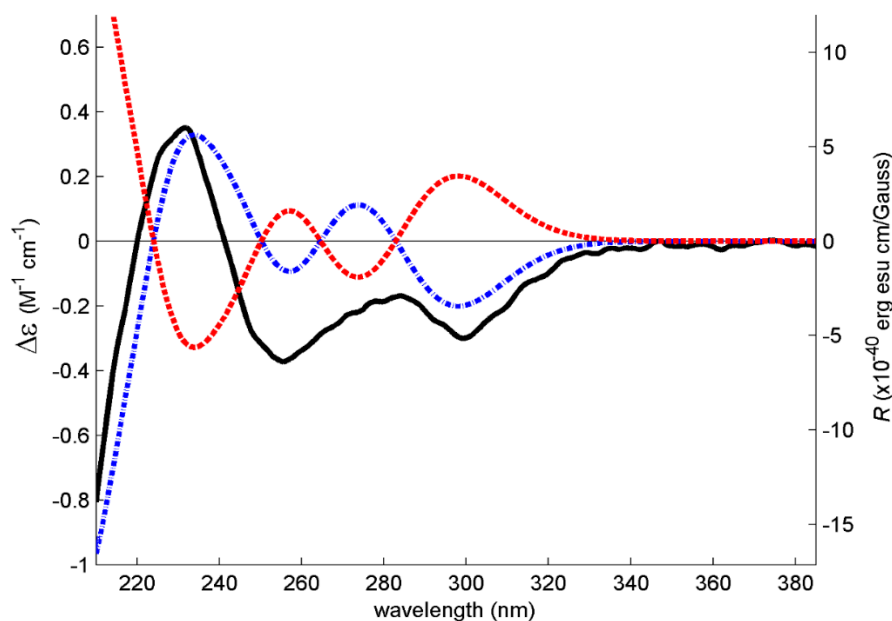


**Figure 5.** Experimental ECD spectrum of **7** in acetonitrile (solid black line) and theoretical ECD spectra of its (*S*) (dot-dashed blue line) and (*R*) (dashed red line) computational models.

Literature search through SciFinder revealed that **7** has never been previously described, and, therefore, was named spinolactone.

Interestingly, Nishida et al. [18] reported the structure of a similar compound containing a 11*H*-dibenzo[*b,e*][1,4]dioxepin-11-one scaffold, named purpactin *C'* which was obtained by conversion of purpactin *C*, isolated from a fermentation broth of *Penicillium purpurogenum* FO-608. However, the authors only presented its HREI-MS, <sup>1</sup>H and <sup>13</sup>C NMR data (CDCl<sub>3</sub>, 300 and 75 MHz) of purpactin *C'*. Later on, Chen et al. isolated purpactin *C'* from a gorgonian-derived *Talaromyces* sp. [19], whereas Daengrot et al. also described the isolation of the same compound from a soil-derived *Penicillium aculeatum* PSU-RSPG105 [16]. In both cases, the authors reported neither its NMR data nor absolute configuration of the stereogenic carbon in the side chain but only referred to the work of Nishida et al. [18].

Since the two benzene rings of **5–8** possess the same substitution patterns, it is clearly that they share the same biosynthetic origin and route. Condensation of acetyl CoA (**I**) and malonyl CoA (**II**) gives an octaketide **III**, which undergoes a cyclization to give an intermediate **IV**. However, instead of enolization, one of the ketone carbonyl in ring C undergoes a reduction to form a secondary alcohol, which, after oxidation of the methylene group in ring B, gives rise to **VI**. Decarboxylation of ring A and dehydration of the secondary alcohol in ring C of **VI** gives rise to the anthraquinone **VII**. Prenylation on the activated carbon in **VII** by dimethylallyl pyrophosphate (DMAPP) gives rise to a prenyl intermediate **VIII**, followed by enolization to give an intermediate **IX**. Methylation of the phenolic hydroxyl group, *ortho* to the prenyl group, by SAM, leads to the formation of **X**. Oxidative cleavage of the anthraquinone ring gives rise to **XI**. Rotation of the bond between the benzene ring (A) and the carbonyl group in **XI** to **XII** allows a nucleophilic substitution of the hydroxyl group to give an intermediate **XIII**. Oxidation of the aldehyde to a carboxylic acid and oxidation of the double bond of the prenyl side chain lead to an intermediate **XIV**, which, after dehydration, gives **XV**. Regiospecific hydration of the double bond of the side chain of **XV** gives **XVI**, which, after reduction of one of the carboxylic acid group to aldehyde, results in a formation of **XVII**. Acetylation of the hydroxyl group of the side chain leads to the formation of **5**, which, after reduction of the carbonyl carbon of the acetyl group, gives rise to **6** (Figure 6).

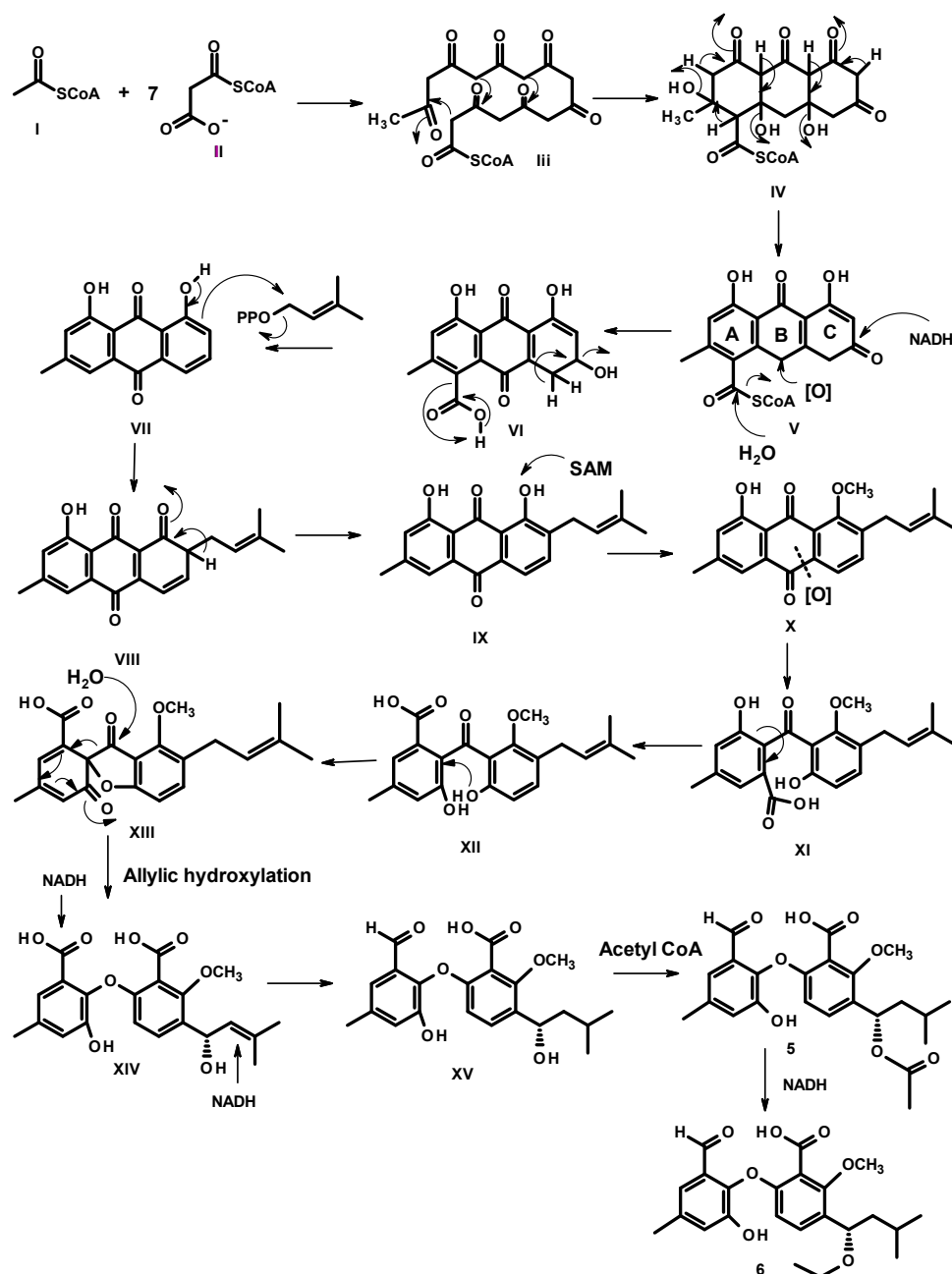


**Figure 6.** Proposed biogenesis of 5 and 6.

Reduction of the aldehyde group on ring A of XVII to a primary alcohol in XVIII or XIX, followed by esterification of the carboxyl group by the phenolic hydroxyl group (in XIX) or by a hydroxyl group of the primary alcohol (in XVIII) leads to the formation of 7 and 8, respectively (Figure 7).

The antimicrobial activity of 2 and 5–8 was evaluated against several reference bacterial species and multidrug-resistant isolates (Table 4); however, only 7 exhibited antibacterial activity against *Enterococcus faecalis* B3/101 with a MIC value of 64 µg/mL (Table 4). The MBC was more than one-fold higher than the MIC, suggesting a bacteriostatic effect.

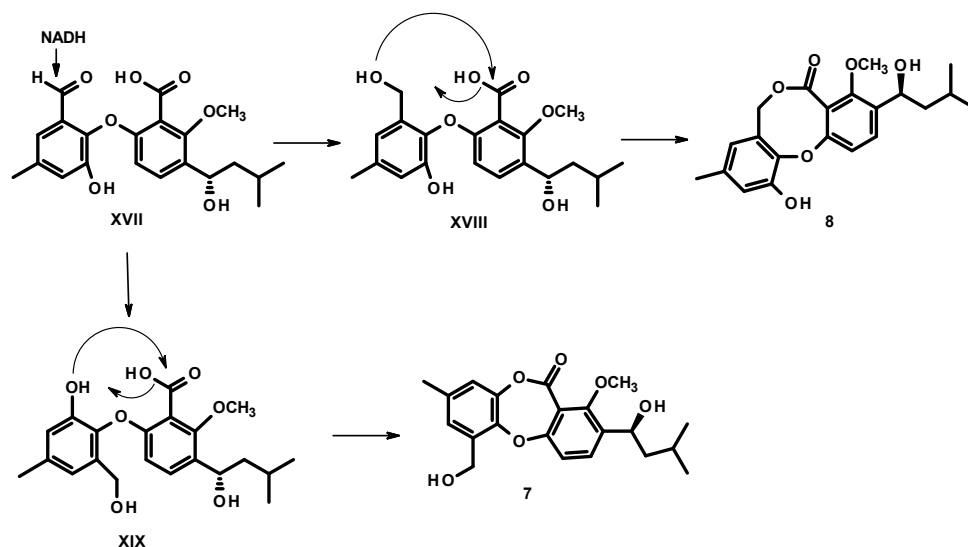


Figure 7. Proposed biogenesis of 7 and 8.

Table 4. Antibacterial activity of 2 and 5–8 against Gram-positive reference and multidrug-resistant strains. MIC is expressed in  $\mu\text{g/mL}$ . Ceftazidime and kanamycin were used as positive controls.

Compound	<i>E. faecalis</i> ATCC 29212	<i>E. faecalis</i> B3/101 (VRE)	<i>S. aureus</i> ATCC 29213	<i>S. aureus</i> 66/1 (MRSA)
2	>64	>64	>64	>64
5	>64	>64	>64	>64
6	>64	>64	>64	>64
7	>64	64	>64	>64
8	>64	>64	>64	>64
CAZ	-	-	8	-
KAN	32	-	-	-

MIC, minimal inhibitory concentration. CAZ, ceftazidime. KAN, kanamycin.

Although 5 and 6 did not exhibit antibacterial activity, they were able to significantly inhibit biofilm formation in three of the four reference strains used in this study (Table 5): *Escherichia coli* ATCC 25922 (both 5 and 6), *Staphylococcus aureus* ATCC 29213 (both 5 and 6), and *E. faecalis* ATCC 29212 (5). A more extensive effect was found for 6, which displayed the strongest inhibitory activity ( $56.00 \pm 0.06$ ) (mean  $\pm$  SD) in *S. aureus* ATCC 29213.

Table 5. Percentage of biofilm formation for compounds that showed antibiofilm activity after 24 h incubation.

Compound	Concentration ( $\mu\text{g/mL}$ )	Biofilm Biomass (% of Control)		
		<i>E. coli</i> ATCC 25922	<i>E. faecalis</i> ATCC 29212	<i>S. aureus</i> ATCC 29213
5	64	$88.39 \pm 0.09$ ***	$75.89 \pm 0.10$ ***	$84.46 \pm 0.10$ ***
6	64	$83.89 \pm 0.19$ ***	-	$56.00 \pm 0.06$ ***

Data are shown as mean  $\pm$  SD of three independent experiments. One-sample *t*-test: \*\*\*  $p < 0.001$  significantly different from 100%. MIC, minimal inhibitory concentration.

This result led us to investigate the influence of 6 in both biofilm viability (Figure 8) and its matrix spatial arrangement (Figure 9). After 8 h of incubation, the viability of the biofilm of *S. aureus* ATCC 29213 was significantly affected by 6, exhibiting a percentage of control of  $1.80 \pm 0.0014$ , representing a viability reduction of 98%. On the contrary, after 24 h of incubation, the percentage of control increased to  $89.65 \pm 0.0021$ , showing only a

10% viability reduction. Although the results herein presented suggest a sublethal effect of **6** on a specific molecular or structural target of *S. aureus*, that could be reversed over time due to genetic and phenotypic adaptability of bacteria; however, it cannot be ruled out that the compound may undergo some degradation or biodegradation. Further studies are warranted to shed more light on this subject.

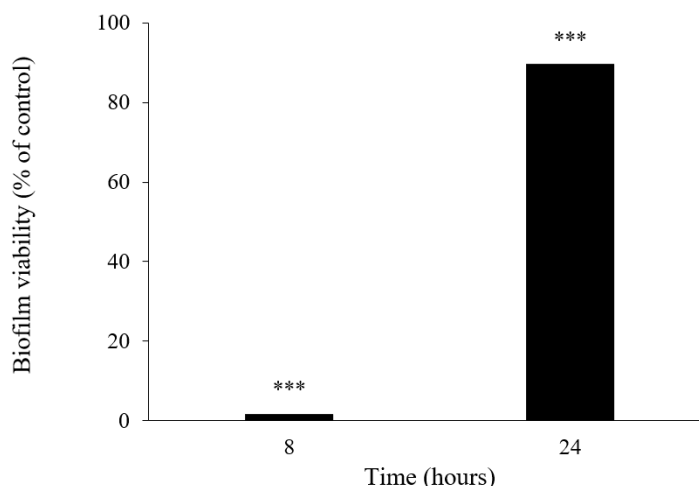


**Figure 8.** Biofilm viability effect in *S. aureus* ATCC 29213 in the presence of **6** after 8 and 24 h of incubation. Where \*\*\* represent statistical significance of data as  $p < 0.001$ .

Regarding the effect on biofilm extracellular polymeric substances, **6** caused an increased number of channels, homogeneously distributed by the biofilm, after 8 h of incubation (Figure 9). However, after 24 h of incubation, this biofilm did not maintain its structure, appearing quite similar to the control (data not shown). In fact, *S. aureus* ATCC 29213 typically produces a dense biofilm structure with lower number of observed channels. Biofilm interstitial voids (channels) are physiologically relevant for diffusion and circulation of nutrients, oxygen and essential substances. Factors such as cell-to-cell communication and alterations in attachment of bacterial cell to surfaces can influence the dynamic of biofilm, namely the evolution of the channels. Formation of channels was shown to be affected by molecules like surfactants, which have the ability to modulate gene expression and to maintain open channels [20,21]. Nonetheless, the present study highlights the promising results of **6** in *S. aureus* biofilm early development. Understanding the antibiofilm dynamic in the presence of **6** and its stability is essential to evaluate its activity, especially within the first 8 h of incubation. Compound **5** was also investigated for its potential synergy with clinically relevant antibiotics on the multidrug-resistant isolates, by both disk diffusion method and checkerboard assay; however, no interactions were observed.

Compounds **2** and **5–8** were also tested for their *in vitro* acetylcholinesterase (AChE) inhibitory activity by a modified Ellman's method [22]; however, none of the tested compounds showed inhibition of the enzyme at concentrations as high as 80  $\mu\text{M}$  (a positive control galantamine showed a percentage inhibition of 94.82% at 80  $\mu\text{M}$ , and an  $\text{IC}_{50}$  value of 16.76  $\mu\text{M}$ ). Additionally, **2** and **5–8** were also evaluated for their anti-tyrosinase activity at the maximum concentration of 200  $\mu\text{M}$  by using a modified microplate assay as described previously [23]. All the tested compounds, except **6**, inhibited tyrosinase activity. However, as **8** showed a percentage of inhibition higher than 50% at 200  $\mu\text{M}$ , its  $\text{IC}_{50}$  value ( $177.03 \pm 8.17 \mu\text{M}$ ) was obtained at lower doses (i.e., 150 and 100  $\mu\text{M}$ ), indicating its moderate anti-tyrosinase activity. On the contrary, **2**, **5**, **7** showed weak inhibitory effects. Table 6 shows percent inhibition at 200  $\mu\text{M}$  and  $\text{IC}_{50}$  values ( $\mu\text{M}$ ) of the tested compounds.

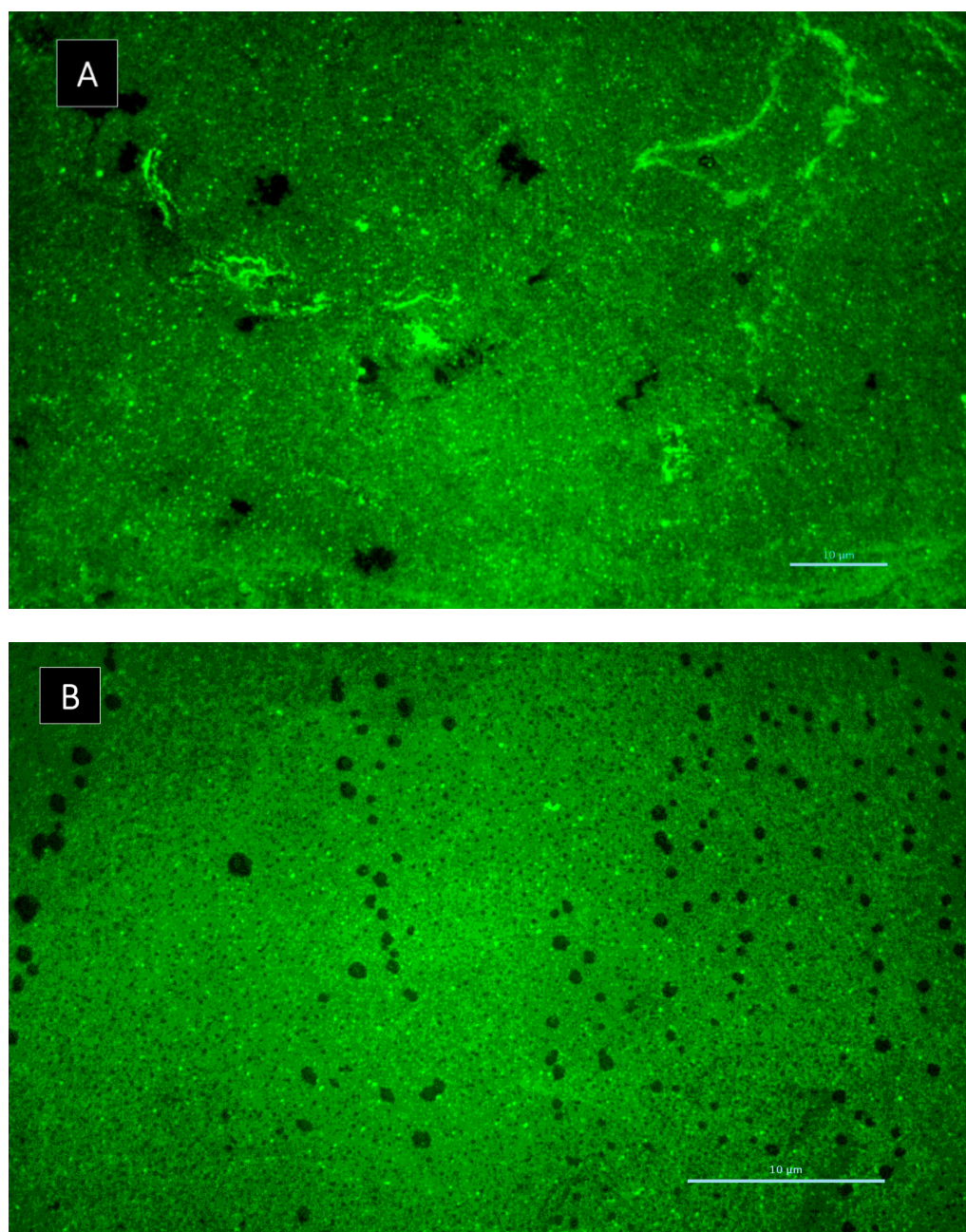


**Figure 9.** Rhodamine-conA staining of *S. aureus* ATCC 29213 biofilm: (A) in the absence of 6 and (B) in the presence of 6 after 8 h incubation. Scale bar = 10 µm. Amplification 1000×.

**Table 6.** Tyrosinase inhibitory activity of 2 and 5–8.

Compounds	% Inhibition at 200 µM	IC <sub>50</sub> (µM)
2	11.56 ± 2.05 *	n.d.
5	4.58 ± 0.07 ***	n.d.
6	n.a.	-
7	5.33 ± 0.18 ***	n.d.
8	53.1 ± 1.17 ***	177.03 ± 8.17 **
Kojic acid (positive control)	95.04 ± 0.018 ****	14.00 ± 0.12 ****

Results are given as mean ± SEM of three independent experiments performed in triplicate; n.a.: not active; n.d.: not determined;  $p < 0.05$  (\*);  $p < 0.01$  (\*\*);  $p < 0.001$  (\*\*\*) ;  $p < 0.0001$  (\*\*\*\*).

### 3. Experimental Section

#### 3.1. General Experimental Procedures

The melting points were determined on a Stuart Melting Point Apparatus SMP3 (Bibby Sterilin, Stone, Staffordshire, UK) and are uncorrected. Optical rotations were measured on an ADP410 Polarimeter (Bellingham + Stanley Ltd., Tunbridge Wells, Kent, UK).  $^1\text{H}$  and  $^{13}\text{C}$  NMR spectra were recorded at ambient temperature on a Bruker AMC instrument (Bruker Biosciences Corporation, Billerica, MA, USA) operating at 300 or 500 and 75 or 125 MHz, respectively. High-resolution mass spectra were measured with a Waters Xevo QToF mass spectrometer (Waters Corporation, Milford, MA, USA) coupled to a Waters Aquity UPLC system. A Merck (Darmstadt, Germany) silica gel GF<sub>254</sub> was used for preparative TLC, and Merck Si gel 60 (0.2–0.5 mm), Li Chroprep silica gel and Sephadex LH 20 were used for column chromatography.

#### 3.2. Fungal Material

The fungus was isolated from a marine sponge *Mycale* sp., which was collected by scuba diving at a depth of 10–15 m from the coral reef at Samae San Island (12°34'36.64'' N 100°56'59.69'' E), Chonburi province, Thailand, in September 2016. The sponge was washed with sterilized seawater three times, and then dried on a sterile filter paper under sterile aseptic condition. The sponge was cut into small pieces (5 × 5 mm), and four pieces were placed on Petri dish plates containing 15 mL potato dextrose agar (PDA) medium mixed with 300 mg/L of streptomycin sulfate and incubated at room temperature for 7 days. The hyphal tips emerging from sponge pieces were individually transferred onto PDA slant.

The fungal strain KUFA 1047 was identified as *Neosartorya spinosa*, based on morphological characteristics. This identification was confirmed by molecular techniques using internal transcribed spacer (ITS) primers. DNA was extracted from young mycelia following a modified Murray and Thompson method [24]. The universal primer pairs ITS1 and ITS4 were used for ITS gene amplification [25]. PCR reactions were conducted on a thermal cycler and DNA sequencing analyses were performed using the dideoxyribonucleotide chain termination method [26] by Macrogen Inc. (Seoul, South Korea). The DNA sequences were edited using FinchTV software and submitted into the BLAST program for alignment and compared with that of fungal species in the NCBI database (<http://www.ncbi.nlm.nih.gov/>, accessed on 15 January 2017). Its gene sequences were deposited in GenBank with an accession number MT814287. The pure cultures were maintained at Kasetsart University Fungal Collection, Department of Plant Pathology, Faculty of Agriculture, Kasetsart University, Bangkok, Thailand.

#### 3.3. Extraction and Isolation

The mycelium plugs of *Neosartorya spinosa* KUFA 1047 were transferred into 500 mL Erlenmeyer flasks containing 200 mL of potato dextrose broth (PDB) and incubated on a rotary shaker at 120 rpm for 7 days at room temperature for preparing a mycelial suspension. Fifty 1 L Erlenmeyer flasks, each containing 300 g sterile cooked rice and then inoculated with 20 mL of mycelial suspension in each flask and incubated at room temperature for 30 days. Then, 500 mL of EtOAc were added to each flask and macerated for 7 days and then filtered with Whatman filter paper N<sup>o</sup>.1 (GE Healthcare UK Limited, Buckinghamshire, UK). The organic solutions were combined and then evaporated under reduced pressure to give 227.8 g of crude EtOAc extracts of *N. spinosa* KUFA 1047. The crude EtOAc extract of *N. spinosa* KUFA 1047 was dissolved in 500 mL of EtOAc and then washed with a 5% NaHCO<sub>3</sub> solution (4 × 250 mL). The resulting organic phase was washed with deionized water (3 × 500 mL) and dried with anhydrous Na<sub>2</sub>SO<sub>4</sub>, filtered, and evaporated under reduced pressure, to obtain 31.2 g of the crude EtOAc extract, which was applied on a column chromatography of silica gel 60 (350 g) and eluted with mixtures of petrol-CHCl<sub>3</sub> and CHCl<sub>3</sub>-Me<sub>2</sub>CO, wherein 250 mL fractions (frs) were collected as follows: frs 1–192 (petrol-CHCl<sub>3</sub>, 3:7), 193–282 (petrol-CHCl<sub>3</sub>, 1:9), 283–432 (CHCl<sub>3</sub>-Me<sub>2</sub>CO, 9:1), and 433–598 (CHCl<sub>3</sub>-Me<sub>2</sub>CO, 7:3). Frs 109–155 were combined (980 mg)

and applied over a column chromatography of Sephadex LH-20 (15 g) and eluted with MeOH, wherein 35 sub-fractions (sfrs) of 1 mL were collected. Sfrs 9–22 were combined (861.5 mg) and applied over a column chromatography of Sephadex LH-20 (15 g) and eluted with CHCl<sub>3</sub>, wherein 22 sfrs of 1 mL were collected. Sfrs 8–13 were combined (483 mg) and applied over a column chromatography of Sephadex LH-20 (5 g) and eluted with MeOH, wherein 14 sfrs of 0.25 mL were collected. Frs 5–9 were combined (237.4 mg) and applied over a column chromatography of Sephadex LH-20 (5 g) and eluted with MeOH, wherein 12 sfrs of 0.25 mL were collected. Sfrs 9–12 were combined and to give 36.9 mg of yellow viscous mass of **8**. Frs 156–200 were combined (180.0 mg) and applied over a column chromatography of Sephadex LH-20 (5 g), and eluted with MeOH, wherein 17 sfrs of 1 mL were collected. Sfrs 8–17 were combined (42.8 mg) and applied over a column chromatography of Sephadex LH-20 (5 g), and eluted with MeOH, wherein 19 sfrs of 0.5 mL were collected. Sfrs 14–19 were combined and to give 5.4 mg of a mixture of **3** and **4**. Sfrs 5–7 (75.5 mg) from the first Sephadex LH-20 column were combined with sfrs 3–13 (36.9) of the second Sephadex LH-20 column (112.4 mg) and applied over a column chromatography of Sephadex LH-20 (5 g), and eluted with CHCl<sub>3</sub>, wherein 22 sfrs of 1 mL were collected. Frs 8–22 were combined (83.6 mg) and purified by TLC (silica gel 60 G<sub>254</sub>, CHCl<sub>3</sub>: Me<sub>2</sub>CO, 9:1) to give 8.8 mg of **7**. Frs 288–291 were combined (226.4 mg) and precipitated in CHCl<sub>3</sub> to give 10.3 mg **2**. The mother liquor (209.8 mg) was applied over a column chromatography of Sephadex LH-20 (5 g) and eluted with MeOH, wherein 29 sfrs of 0.25 mL were collected. Sfrs 8–15 were combined (128.4 mg) and applied over a column chromatography of Sephadex LH-20 (5 g) and eluted with CHCl<sub>3</sub>, wherein 23 sfrs of 1 mL were collected. Sfrs 19–23 were combined (43.2 mg) and purified by TLC (silica gel 60 G<sub>254</sub>, petrol: CHCl<sub>3</sub>: Me<sub>2</sub>CO, 2: 85:13) to give 14.3 mg of **6**. Frs 293–298 were combined (798.7 mg) and precipitated in CHCl<sub>3</sub> to give additional 9.4 mg of **2**. Frs 339–379 were combined (506.6 mg) and purified by TLC (silica gel 60 G<sub>254</sub>, CHCl<sub>3</sub>: Me<sub>2</sub>CO, 85:15). One of the bands from the TLC plates (128.4 mg) was applied over a column chromatography of Sephadex LH-20 (5 g) and eluted with MeOH, wherein 19 sfrs of 0.25 mL were collected. Sfrs 4–19 were combined (108.1 mg) and precipitated in CHCl<sub>3</sub> to give 39.3 mg of **5**. Frs 299–338 (1.29 g), the mother liquor of frs 293–298 (775.9 mg), and the rest of the TLC bands of frs 339–379 (65.1 mg) were combined (2.13 mg) and applied over a column chromatography of Li Chroprep<sup>®</sup> silica gel (35 g) and eluted with mixtures of petrol–CHCl<sub>3</sub> and CHCl<sub>3</sub>–Me<sub>2</sub>CO, wherein 112 sfrs of 100 mL were collected as follow: 1–26 (petrol–CHCl<sub>3</sub>, 3:7), 27–75 (petrol–CHCl<sub>3</sub>, 1:9), 76–99 (CHCl<sub>3</sub>–Me<sub>2</sub>CO, 9:1), and 100–112 (CHCl<sub>3</sub>–Me<sub>2</sub>CO, 7:3). Sfrs 7–8 were combined (41.5 mg) and applied over a column chromatography of Li Chroprep<sup>®</sup> silica gel (8 g) and eluted with mixtures of petrol–CHCl<sub>3</sub> and CHCl<sub>3</sub>–Me<sub>2</sub>CO, wherein 33 sfrs of 25 mL were collected as follow: sfrs 1–4 (petrol–CHCl<sub>3</sub>, 1:1), 5–17 (petrol–CHCl<sub>3</sub>, 3:7), 18–25 (petrol–CHCl<sub>3</sub>, 1:9), 26–30 (CHCl<sub>3</sub>–Me<sub>2</sub>CO, 9:1), and 31–33 (CHCl<sub>3</sub>–Me<sub>2</sub>CO, 7:3). Sfrs 9–11 were combined (7.6 mg) and precipitated in CHCl<sub>3</sub> to give 6.6 mg of **1**.

### 3.3.1. Acetylpenipurdin A (**4**)

For <sup>1</sup>H and <sup>13</sup>C NMR spectroscopic data (CDCl<sub>3</sub>, 300 and 75 MHz), see Table 1. (+)-HRESIMS *m/z* 371.1124 (M + H)<sup>+</sup> (calcd for C<sub>20</sub>H<sub>19</sub>O<sub>7</sub>, 329.1131).

### 3.3.2. Neospinosic Acid (**6**)

Yellow amorphous solid. [ $\alpha$ ]<sub>D</sub><sup>20</sup> -166.7 (*c* = 0.042, MeOH). IR (KBr)  $\nu_{\max}$  3447 (OH), 2956, 2930, 2869, 1683 (CHO), 1653, 1616, 1596, 1472, 1323, and 12792 cm<sup>-1</sup>. For <sup>1</sup>H and <sup>13</sup>C spectroscopic data (DMSO-*d*<sub>6</sub>, 300 and 75 MHz), see Table 2; (+)-HRESIMS *m/z* 417.1915 (M + H)<sup>+</sup> (calcd for C<sub>23</sub>H<sub>29</sub>O<sub>7</sub>, 417.1913); 439.1735 (M + Na)<sup>+</sup> (calcd for C<sub>23</sub>H<sub>28</sub>O<sub>7</sub>Na, 439.1733).

### 3.3.3. Spinolactone (7)

Yellow viscous oil.  $[\alpha]_D^{20}$   $-311.5$  ( $c = 0.06$ , MeOH). IR (KBr)  $\nu_{\max}$  3423 (OH), 2955, 2927, 2868, 1746, 1596, 1521, 1488, 1470, 1225, and 1202  $\text{cm}^{-1}$ . For  $^1\text{H}$  and  $^{13}\text{C}$  spectroscopic data (DMSO- $d_6$ , 500 and 125 MHz), see Table 3; (+)-HRESIMS  $m/z$  373.1652 (M+H) $^+$  (calcd for  $\text{C}_{21}\text{H}_{25}\text{O}_6$ , 373.1651).

### 3.4. Electronic Circular Dichroism (ECD)

The experimental UV and ECD spectra of **5** and **7** (ca. 1 mg/mL in methanol and acetonitrile) were obtained in a Jasco J-815 CD spectropolarimeter (Jasco Europe S.R.L., Cremella, Italy) with a 0.1 mm cuvette and 12 accumulations. The simulated ECD spectrum was obtained by first determining all the relevant conformers of the (S)-**5** computational model. Its conformational space was developed by rotating by 90, 120, or 180 degrees all the single, non-cyclic, bonds, depending on the MM2 torsion energy minima. The large number of conformational degrees of freedom of **5** resulted in a huge number of conformers, which were MM2 minimized with PerkinElmer's Chem3D Ultra 20.1.0.110 (PerkinElmer Inc., Waltham, MA, USA) and ChemScript (PerkinElmer Inc., Waltham, MA, USA) and filtered to eliminate like conformations with VeraChem's Vconf 2.0 (VeraChem LLC, Germantown, MA, USA), resulting in 351 different conformers. Since the MM2 energies of all of these conformers fell within an interval of 3 kcal/mol, many with very similar values, all the 351 conformers were minimized using the semi-empirical method PM6/methanol using Gaussian 16W (Gaussian Inc., Wallingford, NY, USA) and then filtered again. Out of these, 351 PM6 conformers, 20 were found within a 2 kcal/mol interval (about 85% of the population) and were subjected to a final minimization round using the quantum mechanical DFT method B3LYP/6-31G/methanol method (Gaussian 16W), which was also used to calculate its first 70 ECD transitions (TDDFT). The line spectrum for each one of the 20 conformations was built by applying a Gaussian line broadening of 0.3 eV to each computed transition with a constant UV shift of  $-4$  nm. The final ECD spectrum was obtained by the Boltzmann-weighted sum of the 20 line spectra [27].

The simulated ECD spectrum was obtained by first determining all the relevant conformers of the (S)-**7** computational model. Its conformational space was developed by rotating by 45 degrees all the single, non-cyclic, bonds for each of the two possible bends about the 7-cycle oxygens. The resulting conformers (over 1000) were MM2 minimized (with PerkinElmer's Chem3D Ultra) and filtered to eliminate like conformations (with VeraChem's Vconf 2.0). The lowest 104 conformers, representing about 99% of MM2 total conformer energy, were further minimized using the PM6/acetonitrile semi-empirical method (Gaussian Inc.'s Gaussian 16W) and filtered. The lowest 96% PM6 energy conformers (21 models) were subjected to a final minimization round using the quantum mechanical DFT method B3LYP/6-31G/acetonitrile method (Gaussian 16W), which was also used to calculate its first 70 ECD transitions (TDDFT). The line spectrum for each one of the 21 conformations was built by applying a Gaussian line broadening of 0.2 eV to each computed transition with a constant UV shift of  $-5$  nm. The final ECD spectrum was obtained by the Boltzmann-weighted sum of the 21 line spectra [27].

### 3.5. Antibacterial Activity Bioassays

#### 3.5.1. Bacterial Strains and Growth Conditions

Four reference strains obtained from the American Type Culture Collection were included in this study: two Gram-positive (*Staphylococcus aureus* ATCC 29213 and *Enterococcus faecalis* ATCC 29212), two Gram-negative (*Escherichia coli* ATCC 25922 and *Pseudomonas aeruginosa* ATCC 27853), and one clinical isolate (*E. coli* SA/2, an extended-spectrum  $\beta$ -lactamase producer-ESBL) and two environmental isolates: *S. aureus* 74/24 [28], a methicillin-resistant isolate (MRSA), and *E. faecalis* B3/101 [29] a vancomycin-resistant (VRE) isolate. All bacterial strains were cultured in MH agar (MH-BioKar Diagnostics, Allone, France) and incubated overnight at 37 °C before each assay, in order to obtain fresh cultures. Stock solutions of the compounds were prepared in dimethyl sulfoxide (DMSO—

Alfa Aesar, Kandel, Germany), kept at  $-20\text{ }^{\circ}\text{C}$ , and freshly diluted in the appropriate culture media before each assay. All stock solutions were prepared at final concentration of  $10\text{ mg/mL}$  and, in all experiments, in-test concentrations of DMSO were kept below 1%, as recommended by the Clinical and Laboratory Standards Institute [30].

### 3.5.2. Antimicrobial Susceptibility Testing

The Kirby–Bauer method was used to screen the antimicrobial activity of the compounds according to CLSI recommendations [31]. Briefly, sterile blank paper disks with 6 mm diameter (Liofilchem, Roseto degli Abruzzi, TE, Italy) were impregnated with  $15\text{ }\mu\text{g}$  of each compound and placed on MH plates previously inoculated with a bacterial inoculum equal to 0.5 McFarland turbidity. Blank paper disks impregnated with DMSO were used as negative control. MH inoculated plates were incubated for 18–20 h at  $37\text{ }^{\circ}\text{C}$  and afterwards the diameter of the inhibition zones was measured in mm.

Minimal inhibitory concentrations (MIC) were determined by the broth microdilution method, as recommended by the CLSI [32]. Two-fold serial dilutions of the compounds were prepared in cation-adjusted Mueller–Hinton broth (CAMHB- Sigma-Aldrich, St. Louis, MO, USA). The tested concentrations ranged from 1 to  $64\text{ }\mu\text{g/mL}$ , in order to keep in-test concentrations of DMSO below 1%, avoiding bacterial growth inhibition. Colony-forming unit counts of the inoculum were conducted to ensure that the final inoculum size closely approximated the intended number ( $5 \times 10^5\text{ CFU/mL}$ ). The 96-well U-shaped untreated polystyrene plates were incubated for 16–20 h at  $37\text{ }^{\circ}\text{C}$  and the MIC was determined as the lowest concentration of compound that prevented visible growth. During the essays, ceftazidime hidrate (CAZ, Sigma-Aldrich, St. Louis, MO, USA) and kanamycin monosulfate (KAN, Duchefa Biochemie, Haarlem, The Netherlands) were used as positive control of *S. aureus* ATCC 29213 and *E. faecalis* ATCC 29212, respectively. The minimal bactericidal concentration (MBC) was determined by spreading  $10\text{ }\mu\text{L}$  of the content of the wells with no visible growth on MH plates. The MBC was determined as the lowest concentration of compound at which no colonies grew after overnight incubation at  $37\text{ }^{\circ}\text{C}$  [33]. At least three independent assays were conducted for reference and multidrug-resistant strains.

### 3.5.3. Antibiotic Synergy Testing

To evaluate the combined effect of the compounds tested with clinically relevant antibacterial drugs, the Kirby–Bauer method was used, as previously described [34]. A set of antibiotic disks (Oxoid, Basingstoke, UK), to which the isolates were resistant, was selected: cefotaxime (CTX,  $30\text{ }\mu\text{g}$ ) for *E. coli* SA/2, vancomycin (VAN,  $30\text{ }\mu\text{g}$ ) for *E. faecalis* B3/101, and oxacillin (OXA,  $1\text{ }\mu\text{g}$ ) for *S. aureus* 66/1. Antibiotic disks impregnated with  $15\text{ }\mu\text{g}$  of each compound were placed on seeded MH plates. The controls used included antibiotic disks alone, blank paper disks impregnated with  $15\text{ }\mu\text{g}$  of each compound alone, and blank disks impregnated with DMSO. Plates with CTX were incubated for 18–20 h and plates with VAN and OXA were incubated for 24 h at  $37\text{ }^{\circ}\text{C}$  [30]. Potential synergy was considered when the inhibition halo of an antibiotic disk impregnated with compound was greater than the inhibition halo of the antibiotic or compound-impregnated blank disk alone.

The combined effect of the compounds and clinically relevant antimicrobial drugs was also evaluated by determining the antibiotic MIC in the presence of each compound. Briefly, when it was not possible to determine an MIC value for the test compound, the MIC of CTX (Duchefa Biochemie, Haarlem, The Netherlands), VAN (Oxoid, Basingstoke, England), and OXA (Sigma-Aldrich, St. Louis, MO, USA) for the respective multidrug-resistant strain was determined in the presence of the highest concentration of each compound tested in previous assays ( $64\text{ }\mu\text{g/mL}$ ). The antibiotic tested was serially diluted, whereas the concentration of each compound was kept fixed. Antibiotic MICs were determined as described above. Potential synergy was considered when the antibiotic MIC was lower in the presence of compound [35]. Fractional inhibitory concentrations (FIC) were

calculated as follows: FIC of compound = MIC of compound combined with antibiotic/MIC compound alone, and FIC antibiotic = MIC of antibiotic combined with compound/MIC of antibiotic alone. The FIC index (FICI) was calculated as the sum of each FIC and interpreted as follows:  $FICI \leq 0.5$ , “synergy”;  $0.5 < FICI \leq 4$ , “no interaction”;  $4 < FICI$ , “antagonism” [36].

#### 3.5.4. Biofilm Formation Inhibition Assay

The antibiofilm activity of compounds was evaluated through quantification of total biomass, using the crystal violet method, as previously described [34,37]. Briefly, the highest concentration of compound tested in the MIC assay was added to bacterial suspensions of  $1 \times 10^6$  CFU/mL prepared in unsupplemented Tryptone Soy broth (TSB, Biokar Diagnostics, Allone, Beauvais, France) or TSB supplemented with 1% (*p/v*) glucose (D-(+)-glucose anhydrous for molecular biology, PanReac AppliChem, Barcelona, Spain) for Gram-positive strains. When it was possible to determine a MIC, concentrations ranging from  $2 \times \text{MIC}$  to  $\frac{1}{4} \text{MIC}$  were tested, while keeping in-test concentrations of DMSO below 1%. When it was not possible to determine a MIC, the concentration tested was 64  $\mu\text{g/mL}$ . Controls with appropriate concentration of DMSO, as well as a negative control (TSB or TSB+1% glucose alone), were included. Sterile 96-well flat-bottomed untreated polystyrene microtiter plates were used. After a 24 h incubation at 37 °C, the biofilms were heat-fixed for 1 h at 60 °C and stained with 0.5% (*v/v*) crystal violet (Química Clínica Aplicada, Amposta, Spain) for 5 min. The stain was resolubilized with 33% (*v/v*) acetic acid (acetic acid 100%, AppliChem, Darmstadt, Germany) and the biofilm biomass was quantified by measuring the absorbance of each sample at 570 nm in a microplate reader (Thermo Scientific Multiskan<sup>®</sup> FC, Thermo Fisher Scientific, Waltham, MA, USA). The background absorbance (TSB or TSB+1% glucose without inoculum) was subtracted from the absorbance of each sample and the data are presented as percentage of control. Three independent assays were performed for reference strains, with triplicates for each experimental condition.

#### 3.5.5. Biofilm Viability Assay

Considering the antibiofilm potential of **6**, the metabolic activity of *S. aureus* ATCC 29213 biofilm in presence of **6** at a concentration of 64  $\mu\text{g/mL}$  was assessed using MTT (3-(4,5-dimethylthiazol-2-yl)-2,5-diphenyltetrazolium bromide) assay, as described previously [38,39]. Static biofilm was grown by inoculating  $1 \times 10^6$  CFU/mL bacteria in sterile 96-well flat-bottomed untreated polystyrene microtiter plates containing TSB supplemented with 1% (*w/v*) glucose with a positive and a negative controls. After 8 h and 24 h of incubation at 37 °C, non-adherent cells were removed and 100  $\mu\text{L}$  of MTT (5 mg/mL) (Thiazolyl Blue tetrazolium bromide 98%, Alfa Aesar, Kandel, Germany) was added to each well for 2 h at 37 °C. Thereafter, a solubilization solution (16% (*w/v*) of sodium dodecyl sulfate (SDS for molecular biology, PanReac AppliChem, Barcelona, Spain) and 50% DMSO (*v/v*) were added to dissolve the formazan product into a colored solution. After overnight dissolution at room temperature, biofilm viability was estimated by measuring absorbance of each sample at 570 nm in a microplate reader (Thermo Scientific Multiskan<sup>®</sup> FC, Thermo Fisher Scientific, Waltham, MA, USA). Biofilm viability was expressed as percentage of control and at least two different experiments were performed in triplicate.

#### 3.5.6. Biofilm Matrix Visualization

To visualize the extracellular polymeric substances (EPS) matrix of the biofilms, rhodamine-labeled concanavalin A (rhodamine-conA) (Vector Laboratories, Burlingame, CA, USA), which specifically binds to D-(+)-glucose and D-(+)-mannose residues on exopolysaccharide (EPS), was used, as previously described [40]. Interaction between **6** at a concentration of 64  $\mu\text{g/mL}$  and the biofilm of *S. aureus* ATCC 29213 was selected for rhodamine-conA staining, as a consequence of its antibiofilm potential. Briefly, bacterial suspensions of  $1 \times 10^6$  CFU/mL prepared in TSB supplemented with 1% (*w/v*) glucose was added to a sterile well chamber (Ibidi, Gräfelfing, Germany). After 8 h of incubation,

non-adherent cells were removed from each well and washed with 200  $\mu\text{L}$  of PBS. Then, 100  $\mu\text{L}$  of a rhodamine-conA (10 mg/mL) solution was added to the biofilm for 30 min in the dark at room temperature. Thereafter, the biofilm was washed with 200  $\mu\text{L}$  of PBS and microscopic visualization, using an excitation of 514 nm and an emission wavelength of  $600 \pm 50$  nm.

### 3.6. Acetylcholinesterase Inhibitory Activity Assay

AChE inhibitory assay was performed according to the Ellman's method [22]. Briefly, 20  $\mu\text{L}$  of 0.22 U/mL AChE in tris buffer (50 mM, pH 8.0) from *Electrophorus electricus* (EC 3.1.1.7, Sigma-Aldrich, St. Louis, MO, USA) was added to the wells containing 10  $\mu\text{L}$  of tested compounds (80  $\mu\text{M}$  in DMSO), 100  $\mu\text{L}$  of 3 mM of 5,5'-dithio-bis-(2-nitrobenzoic acid) (DTNB, Sigma-Aldrich, St. Louis, MO, USA) (in 50 mM tris buffer, pH 8.0), 20  $\mu\text{L}$  of 15 mM acetylthiocholine iodide (Sigma-Aldrich, St. Louis, MO, USA) (in 50 mM tris buffer, pH 8.0), and 100  $\mu\text{L}$  of 50 mM tris buffer (pH 8.0). Absorbance of the colored-end product was measured at 412 nm for 5 min, with 30 s intervals (BioTek Synergy™ HT Microplate Reader, Winooski, VT, USA). Controls containing 10  $\mu\text{L}$  of DMSO instead of the tested compounds and reaction blanks containing 20  $\mu\text{L}$  of buffer (0.1% (w/v) bovine serum albumin in 50 mM Tris-HCl) instead of the enzyme and 10  $\mu\text{L}$  of DMSO instead of the tested compounds were made. In this assay, sample blanks containing 20  $\mu\text{L}$  of buffer (0.1% (w/v) bovine serum albumin in 50 mM Tris-HCl) instead of AChE were also performed. The percentage of enzymatic inhibition was calculated as:

$$\text{Percentage inhibition} = 100 - [(S - S_0)/(C - C_0)] \times 100$$

where  $C$  is the absorbance of the control,  $C_0$  is the absorbance of reaction blank,  $S$  is the absorbance in the presence of the tested compounds, and  $S_0$  is the absorbance of sample blanks. All experiments were done in triplicate and galantamine (Sigma-Aldrich, St. Louis, MO, USA), tested at concentrations of 80, 10, 5, and 3.6  $\mu\text{M}$  in DMSO, was used as a positive control as well as for validating the method. The inhibitory activities of the tested compounds toward AChE were expressed as percentage of inhibition as indicated previously. The  $\text{IC}_{50}$  value of galantamine was obtained by interpolation from a linear regression analysis.

### 3.7. Tyrosinase Inhibitory Activity Assay

Tyrosinase inhibitory assay was performed according to the method previously described [23]. Briefly, 20  $\mu\text{L}$  of the mushroom tyrosinase (EC 1.14.18.1, Sigma-Aldrich, St. Louis, MO, USA, 480 U/mL) in 20 mM phosphate buffer was added to the wells containing 20  $\mu\text{L}$  of the tested compounds (200  $\mu\text{M}$  in DMSO), and 140  $\mu\text{L}$  of 20 mM phosphate buffer (pH 6.8). After incubation at 25 °C for 10 min, 20  $\mu\text{L}$  of 0.85 mM L-DOPA (Sigma-Aldrich, St. Louis, MO, USA) in phosphate buffer (pH 6.8) was added and the absorbance of the colored-end product was measured at 25 °C, 11 times for 10 min., with 1 min. intervals at 475 nm (BioTek Synergy™ HT Microplate Reader, Winooski, VT USA). Controls containing 20  $\mu\text{L}$  of DMSO instead of the tested compounds, and reaction blanks containing 20  $\mu\text{L}$  of 20 mM phosphate buffer (pH 6.8) instead of tyrosinase, and 20  $\mu\text{L}$  of DMSO instead of the tested compounds were performed. Moreover, sample blanks containing 20  $\mu\text{L}$  of 20 mM phosphate buffer (pH 6.8) instead of tyrosinase were made. The percentage inhibition of tyrosinase activity was calculated as:

$$\text{Percentage inhibition} = 100 \times [1 - (S - S_0)/(C - C_0)]$$

where  $S$  is the absorbance in presence of the tested compounds,  $S_0$  is the absorbance of sample blanks,  $C$  is the absorbance of the control, and  $C_0$  is the absorbance of reaction blank. All experiments are done in triplicate and kojic acid (Sigma-Aldrich, Saint Louis, MO, USA) at concentrations of 200, 100, 25, 12.5, 8 and 5  $\mu\text{M}$  was used as a positive control. The inhibitory activities of the compounds towards tyrosinase were expressed as

per-centage of inhibition as indicated previously. The IC<sub>50</sub> value of kojic acid was obtained by interpolation from a linear regression analysis.

### 3.8. Statistical Analysis

Data were reported as means  $\pm$  standard error of the mean (SEM) of at least three independent experiments. Statistical analysis of the results was performed with GraphPad Prism (GraphPad Software, San Diego, CA, USA). Unpaired *t*-test was carried out to test for any significant differences between the means. Differences at the 5% confidence level were considered significant.

## 4. Conclusions

The EtOAc extract from a solid culture of a marine-derived fungus *Neosartorya spinosa* KUFA1047, isolated from a marine sponge *Mycale* sp. collected in the Gulf of Thailand, furnished five previously reported secondary metabolites *viz.* (*R*)-6-hydroxymellein (**1**), penipurdin A (**2**), acetylquestinol (**3**), tenellic acid C (**5**) and vermioxin A (**8**), in addition to three previously unreported compounds, including acetylpenipurdin A (**4**), neospinosic acid (**6**), and spinolactone (**7**). All the isolated compounds, except **1**, were assayed for *in vitro* anticholinesterase and anti-tyrosinase activities. Although none of the test compounds exhibited anticholinesterase activity, **2**, **5**, and **7** exhibited weak anti-tyrosinase activity, while **8** showed moderate inhibitory activity against a mushroom tyrosinase. Compounds **2** and **5–8** were also assayed for their antibacterial activity against several reference bacterial species and multidrug-resistant isolates; however, only **7** exhibited antibacterial activity against *Enterococcus faecalis* B3/101 with a MIC value of 64  $\mu$ g/mL. Since the MBC was more than one-fold higher than the MIC, **7** was suggested to exert a bacteriostatic effect. Interestingly, although **5** and **6** did not exhibit antibacterial activity, they were able to significantly inhibit biofilm formation in three of the four reference strains used in this study. While both **5** and **6** inhibited biofilm formation in *Escherichia coli* ATCC 25922 and *Staphylococcus aureus* ATCC 29213, only **5** inhibited biofilm formation in *E. faecalis* ATCC 29212. Interestingly, **6** exerts more extensive effect, displaying the strongest inhibitory activity in *S. aureus* ATCC 29213. In summary, secondary metabolites isolated from this marine-derived fungus are more preponderant in antibacterial and antibiofilm activities than anticholinesterase activity.

**Supplementary Materials:** The following are available online at <https://www.mdpi.com/article/10.3390/md19080457/s1>: Figures S1–S5, S7–S11, S13–S17, S20–S24, S26–S30, S32–S36, and S38–S42: 1D and 2D NMR spectra of compounds **1–8**. Figures S6, S12, S18, S19, S25, S31, S37, and 43: HRMS data for compounds **1–8**. Table S1: <sup>1</sup>H and <sup>13</sup>C NMR (DMSO-*d*<sub>6</sub>, 300 and 75 MHz) and HMBC assignment for **1**; Table S2. <sup>1</sup>H and <sup>13</sup>C NMR (DMSO-*d*<sub>6</sub>, 300 and 75 MHz) and HMBC assignment for **2**; Table S3. <sup>1</sup>H and <sup>13</sup>C NMR (DMSO-*d*<sub>6</sub>, 500 and 125 MHz) and HMBC assignment for **3**; Table S4. <sup>1</sup>H and <sup>13</sup>C NMR (300 and 75 MHz, DMSO-*d*<sub>6</sub>) and HMBC assignment of **5**; Table S5. <sup>1</sup>H and <sup>13</sup>C NMR (300 and 75 MHz, CDCl<sub>3</sub>) and HMBC assignment of **8**.

**Author Contributions:** A.K. and M.E.S. conceived and designed the experiment and elaborated the manuscript; J.D.M.d.S. performed isolation, purification, and part of structure elucidation of the compounds; T.D. collected, isolated, identified, and cultured the fungus; J.A.P. performed calculations and measurement of ECD spectra and interpretation of the results; H.C. designed and interpreted the result of anticholinesterase and anti-tyrosinase assays; I.C.R. and P.M.C. performed antibacterial and antibiofilm assays; S.M. provided HRMS; A.M.S.S. provided NMR spectra. All authors have read and agreed to the published version of the manuscript.

**Funding:** This work was funded by the structured program of R&D&I ATLANTIDA—Platform for the monitoring of the North Atlantic Ocean and tools for the sustainable exploitation of the marine resources (reference NORTE-01-0145-FEDER-000040), supported by the North Portugal Regional Operational Programme (NORTE2020), through the European Regional Development Fund (ERDF).

**Institutional Review Board Statement:** Not applicable.

**Informed Consent Statement:** Not applicable.

**Acknowledgments:** We thank Sara Cravo for technical assistance for anticholinesterase and anti-tyrosinase assays. The authors acknowledge the support of the Biochemical and Biophysical Technologies i3S Scientific Platform with the assistance of Frederico Silva and Maria de Fátima Fonseca for the access of Jasco J-815 CD spectropolarimeter.

**Conflicts of Interest:** The authors declare no conflict of interest.

## References

1. Brakhage, A.A. Regulation of fungal secondary metabolism. *Nat. Rev. Microbiol.* **2013**, *11*, 21–32. [[CrossRef](#)]
2. Beekman, A.M.; Barrow, R.A. Fungal Metabolites as Pharmaceuticals. *Aust. J. Chem.* **2014**, *67*, 827–843. [[CrossRef](#)]
3. Bugni, T.S.; Ireland, C.M. Marine-derived fungi: A chemically and biologically diverse group of microorganisms. *Nat. Prod. Rep.* **2004**, *21*, 143–163. [[CrossRef](#)] [[PubMed](#)]
4. Prompanya, C.; Fernandes, C.; Cravo, S.; Pinto, M.M.M.; Dethoup, T.; Silva, A.M.S.; Kijjoo, A. A new cyclic hexapeptide and a new isocoumarin derivative from the marine sponge-associated fungus *Aspergillus similanensis* KUFA 0013. *Mar. Drugs* **2015**, *13*, 1432–1450. [[CrossRef](#)]
5. May Zin, W.W.; Prompanya, C.; Buttachon, S.; Kijjoo, A. Bioactive secondary metabolites from a Thai collection of soil and marine-derived fungi of the genera *Neosartorya* and *Aspergillus*. *Curr. Drug Deliv.* **2016**, *13*, 378–388. [[CrossRef](#)]
6. Kumla, D.; Aung, T.S.; Buttachon, S.; Dethoup, T.; Gales, L.; Pereira, J.A.; Inácio, Â.; Costa, P.M.; Lee, M.; Sekeroglu, N.; et al. A New Dihydrochromone Dimer and Other Secondary Metabolites from Cultures of the Marine Sponge-Associated Fungi *Neosartorya fennelliae* KUFA 0811 and *Neosartorya tsunodae* KUFC 9213. *Mar. Drugs* **2017**, *15*, 375. [[CrossRef](#)] [[PubMed](#)]
7. Lucinda, J.; Bessa, L.J.; Buttachon, S.; Dethoup, T.; Martins, R.; Vasconcelos, V.; Kijjoo, A.; Costa, P.M. Neofiscalin A and fiscalin C are potential novel indole alkaloid alternatives for the treatment of multidrug resistant Gram-positive bacterial infections. *FEMS Microbiol. Lett.* **2016**, *363*, fnw150. [[CrossRef](#)]
8. Rajachan, O.-T.; Kanokmedhakul, K.; Sanmanoch, W.; Boonlue, S.; Hannongbua, S.; Saparpakorn, P.; Kanokmedhakul, S. Chevalone C analogues and globoscinic acid derivatives from the fungus *Neosartorya spinosa* KKKU-1NK1. *Phytochemistry* **2016**, *132*, 68–75. [[CrossRef](#)] [[PubMed](#)]
9. May Zin, W.W.; Buttachon, S.; Buaruang, J.; Gale, L.; Pereira, J.A.; Pinto, M.M.M.; Silva, A.M.S.; Kijjoo, A. A new meroditerpene and a new tryptoquivaline analog from the algicolous fungus *Neosartorya takakii* KUFC 7898. *Mar. Drugs* **2015**, *13*, 3776–3790. [[CrossRef](#)] [[PubMed](#)]
10. Islam, M.S.; Ishigami, K.; Watanabe, H. Synthesis of (–)-mellein, (+)-ramulosin, and related natural products. *Tetrahedron* **2007**, *63*, 1074–1079. [[CrossRef](#)]
11. Xue, J.; Fu, Y.; Wu, P.; Xu, L.; Huang, R.; Wei, X.; Li, H. Two new anthraquinones from the soil fungus *Penicillium purpurigenum* SC0070. *J. Antibiot.* **2015**, *68*, 598–599. [[CrossRef](#)]
12. May Zin, W.W.; Buttachon, S.; Dethoup, T.; Pereira, J.A.; Gales, L.; Inácio, Â.; Paulo, M.; Costa, P.M.; Lee, M.; Sekeroglu, N.; et al. Antibacterial and antibiofilm activities of the metabolites isolated from the culture of the mangrove-derived endophytic fungus *Eurotium chevalieri* KUFA0006. *Phytochemistry* **2017**, *141*, 86–97. [[CrossRef](#)]
13. Oh, H.; Kwon, T.O.; Gloer, J.B.; Marvanová, L.; Shearer, S.A. Tenellic Acids A-D: New Bioactive Diphenyl Ether Derivatives from the Aquatic Fungus *Dendrospora tenella*. *J. Nat. Prod.* **1999**, *62*, 580–583. [[CrossRef](#)] [[PubMed](#)]
14. Proksa, B.; Uhrin, D.; Adamcová, J.; Fуска, J. Vermixocins A and B, two novel metabolites from *Penicillium vermiculatum*. *J. Antibiot.* **1992**, *45*, 1268–1272. [[CrossRef](#)]
15. Suzuki, K.; Nozawa, K.; Udagawa, S.; Nakajima, S.; Kawai, K. Penicillide and dehydroisopenicillide from *Talaromyces derxii*. *Phytochemistry* **1991**, *30*, 2096–2098. [[CrossRef](#)]
16. Daengrot, C.; Rukachaisirikul, V.; Tadpetch, K.; Phongpaichit, S.; Bowornwiriyan, K.; Sakayaroj, J.; Shend, X. Penicillanone and penicillidic acids A-C from the soil-derived fungus *Penicillium aculeatum* PSU-RSPG105. *RSC Adv.* **2016**, *6*, 39700. [[CrossRef](#)]
17. Singh, A.J.; Gorka, A.P.; Bokesch, H.R.; Wamiru, A.; O’Keefe, B.R.; Schnermann, M.J.; Gustafson, K.R. Harnessing natural product diversity for fluorophore discovery: Naturally occurring fluorescent hydroxyanthraquinones from the marine crinoid *Pterometra venusta*. *J. Nat. Prod.* **2018**, *81*, 2750–2755. [[CrossRef](#)]
18. Nishida, H.; Tomoda, H.; Cao, J.; Okuda, S.; Omura, S. Purpactins, new inhibitors of acyl-CoA: Cholesterol acyltransferase produced by *Penicillium purpurogenum* II. Structure elucidation of purpactins A, B, C. *J. Antibiot.* **1991**, *44*, 144–151. [[CrossRef](#)]
19. Chen, M.; Han, L.; Shao, C.-L.; She, Z.-G.; Wang, C.-Y. Bioactive diphenyl ether derivatives from a gorgonian-derived fungus *Talaromyces* sp. *Chem. Biodivers.* **2015**, *12*, 443–450. [[CrossRef](#)]
20. Davey, M.E.; Caiazza, N.C.; O’Toole, G.A. Rhamnolipid surfactant production affects biofilm architecture in *Pseudomonas aeruginosa* PAO1. *J. Bacteriol.* **2003**, *185*, 1027–1036. [[CrossRef](#)]
21. Periasamy, S.; Joo, H.-S.; Duong, A.C.; Bach, T.-H.L.; Tan, V.Y.; Chatterjee, S.S.; Cheung, G.Y.C.; Otto, M. How *Staphylococcus aureus* biofilms develop their characteristic structure. *Proc. Natl. Acad. Sci. USA* **2012**, *109*, 1281–1286. [[CrossRef](#)]
22. Ellman, G.L.; Courtney, K.D.; Andres, V., Jr.; Featherstone, R.M. A new and rapid colorimetric determination of acetylcholinesterase activity. *Biochem. Pharmacol.* **1961**, *7*, 88–90. [[CrossRef](#)]
23. Likhitwitayawuid, K.; Sritularak, B. A new dimeric stilbene with tyrosinase inhibitory activity from *Artocarpus gomezianus*. *J. Nat. Prod.* **2001**, *64*, 1457–1459. [[CrossRef](#)]

24. Murray, M.G.; Thompson, W.F. Rapid isolation of high molecular weight plant DNA. *Nucleic Acids Res.* **1980**, *8*, 4321–4325. [[CrossRef](#)]
25. White, T.J.; Bruns, T.; Lee, S.; Taylor, J. Amplification and direct sequencing of fungal ribosomal RNA genes for phylogenetics. In *PCR Protocols: A Guide to Methods and Applications*; Innis, M.A., Gelfand, D.H., Sninsky, J.J., White, T.J., Eds.; Academic Press: New York, NY, USA, 1990; pp. 315–322.
26. Sanger, F.; Nicklen, S.; Coulson, A.R. DNA sequencing with chain-terminating inhibitors. *Proc. Natl. Acad. Sci. USA* **1977**, *72*, 5463–5467. [[CrossRef](#)] [[PubMed](#)]
27. Stephens, P.J.; Harada, N. ECD Cotton effect approximated by the Gaussian curve and other methods. *Chirality* **2010**, *22*, 229–233. [[CrossRef](#)]
28. Simões, R.R.; Aires-de-Sousa, M.; Conceição, T.; Antunes, F.; da Costa, P.M.; de Lencastre, H. High prevalence of EMRSA-15 in Portuguese public buses: A worrisome finding. *PLoS ONE* **2011**, *6*, e17630. [[CrossRef](#)] [[PubMed](#)]
29. Bessa, L.J.; Barbosa-Vasconcelos, A.; Mendes, Â.; Vaz-Pires, P.; Da Costa, P.M. High prevalence of multidrug-resistant *Escherichia coli* and *Enterococcus* spp. in river water, upstream and downstream of a wastewater treatment plant. *J. Water Health* **2014**, *12*, 426–435. [[CrossRef](#)] [[PubMed](#)]
30. CLSI. *Performance Standards for Antimicrobial Susceptibility Testing*, 27th ed.; CLSI supplement M100; Clinical and Laboratory Standards Institute: Wayne, PA, USA, 2017.
31. CLSI. *Performance Standards for Antimicrobial Susceptibility Testing*, 11th ed.; CLSI document M02-A11; Clinical and Laboratory Standards Institute: Wayne, PA, USA, 2012.
32. CLSI. *Methods for Dilution Antimicrobial Susceptibility Tests for Bacteria That Grow Aerobically*, 10th ed.; CLSI document M07-A10; Clinical and Laboratory Standards Institute: Wayne, PA, USA, 2015.
33. CLSI. *Methods for Determining Bactericidal Activity of Antimicrobial Agents*; Approved Guideline, CLSI Document M26-A; Clinical and Laboratory Standards Institute: Wayne, PA, USA, 1999.
34. Kumla, D.; Dethoup, T.; Gales, L.; Pereira, J.A.; Freitas-Silva, J.; Costa, P.M.; Silva, A.; Pinto, M.M.; Kijjoa, A. Erubescensoic Acid, a new polyketide and a xanthonopyrone SPF-3059-26 from the culture of the marine sponge-associated fungus *Penicillium erubescens* KUFA 0220 and antibacterial activity evaluation of some of its constituents. *Molecules* **2019**, *24*, 208. [[CrossRef](#)]
35. Buttachon, S.; Ramos, A.A.; Inácio, Â.; Dethoup, T.; Gales, L.; Lee, M.; Costa, P.M.; Silva, A.M.S.; Sekeroglu, N.; Rocha, E.; et al. Bis-indolyl benzenoids, hydroxypyrrolidine derivatives and other constituents from cultures of the marine sponge-associated fungus *Aspergillus candidus* KUFA0062. *Mar. Drugs* **2018**, *16*, 119. [[CrossRef](#)] [[PubMed](#)]
36. Odds, F.C. Synergy, antagonism, and what the chequer board puts between them. *J. Antimicrob. Chemother.* **2003**, *52*, 1. [[CrossRef](#)]
37. Stepanović, S.; Vuković, D.; Hola, V.; Di Bonaventura, G.; Djukić, S.; Cirković, I.; Ruzicka, F. Quantification of biofilm in microtiter plates: Overview of testing conditions and practical recommendations for assessment of biofilm production by staphylococci. *Apmis* **2007**, *115*, 891–899. [[CrossRef](#)] [[PubMed](#)]
38. Grela, E.; Kozłowska, J.; Grabowiecka, A. Current methodology of MTT assay in bacteria—A review. *Acta Histochem.* **2018**, *120*, 303–331. [[CrossRef](#)] [[PubMed](#)]
39. Riss, T.L.; Moravec, R.A.; Niles, A.L.; Duellman, S.; Benink, H.A.; Worzella, T.J.; Minor, L. Cell viability assays. In *The Assay Guidance Manual [Internet]*; Markossian, S., Grossman, A., Brimacombe, K., Arkin, M., Auld, D., Austin, C.P., Baell, J., Chung, T.D.Y., Coussens, N.P., Dahlin, J.L., et al., Eds.; Eli Lilly & Company and the National Center for Advancing Translational Sciences: Bethesda, MD, USA, 2004; 1 May 2013; Last Update: 1 July 2016. Available online: <https://www.ncbi.nlm.nih.gov/books/NBK144065/> (accessed on 17 June 2021).
40. Bessa, L.J.; Grande, R.; Di Iorio, D.; Di Giulio, M.; Di Campli, E.; Cellini, L. *Helicobacter pylori* free-living and biofilm modes of growth: Behavior in response to different culture media. *Apmis* **2013**, *121*, 149–160. [[CrossRef](#)] [[PubMed](#)]